ACADÉMIE
DES SCIENCES
INSTITUT DE FRANCE

Comptes Rendus
Mécanique

Claude Boutin, Simir Moschini, Francesco d'Annibale and Francesco dell'Isola

From articulated-bi-parallelograms to third gradient 1D continua

Volume 354 (2026), p. 593-619

Online since: 16 June 2026

https://doi.org/10.5802/crmeca.367

The Comptes Rendus. Mécanique *are a member of the Mersenne Center for open scientific publishing*
www.centre-mersenne.org — e-ISSN : 1873-7234

ACADÉMIE DES SCIENCES
INSTITUT DE FRANCE

Comptes Rendus. Mécanique
2026, Vol. 354, p. 593-619
https://doi.org/10.5802/crmeca.367

Research article

From articulated-bi-parallelograms to third gradient 1D continua

Claude Boutin [a,b], **Simir Moschini** [b,c], **Francesco d'Annibale** [b,c] **and Francesco dell'Isola** [b,c]

[a] École Nationale des Travaux publics de l'État — Université de Lyon — LTDS CNRS UMR 5513, Vaulx-en-Velin, France

[b] University of L'Aquila, International Research Center for the Mathematics and Mechanics of Complex Systems, Italy

[c] University of L'Aquila, Department of Civil Construction — Architectural and Environmental Engineering, Italy

E-mails: claude.boutin@entpe.fr, simir.moschini@univaq.it, francesco.dellisola@univaq.it, francesco.dannibale@univaq.it

Abstract. Recently, it has been conjectured that a specific modular articulated bi-parallelogram microstructure is a solution for the problem of synthesis for a 1D continuum whose deformation elastic energy depends on the curvature gradient (dell'Isola et al. [*Math. Mech. Complex Syst.* **12** (2024)] and Terranova et al. [*Comptes Rendus. Mécanique* **353** (2025)]). In this paper, we present an asymptotic procedure for getting the homogenized description of that microstructured system under large in-plane deformation. It is shown that such a periodic structure behaves macroscopically as a third gradient 1D continuum.

The elastic energy stored in a module of such a microstructured system deformed by a gradient of curvature combined with extension is first established. This leads to the energy density of the effective 1D continuum. The latter involves three elastic stiffness coefficients related to the curvature gradient, the elongation, and the coupling of both, whose expressions are explicitly related to the morphology of the module, the stiffnesses of the micro bars, and the curvature.

The strong formulation of the equilibrium condition of the microstructured system is then deduced following the Euler–Lagrange method of minimization of energy. The calculation of the first variation of the deformation energy allows for the determination of the generalized external forces which can be applied to the equivalent 1D continuum whose deformation energy depends on the gradient of curvature and extension: that is, normal and transverse force together with couple and double couple. Consequently, we determine the corresponding balance equations and the constitutive equations for forces and both couple and double couples.

Some numerical examples are given in the case of newly introduced 1D continua loaded at their extremity by couples and double couples.

Keywords. Metamaterials, mechanism, third gradient continua, gradient of curvature, homogenization.

Funding. This work was carried out at the Department of Civil, Building, Architectural and Environmental Engineering of the University of L'Aquila as part of the departmental development project for the five-year period 2023–2027, funded under the "Departments of Excellence" program for the period 2023–2027 (MUR Note No. 15659 of 28 December 2022).

Manuscript received 14 February 2026, revised 23 April 2026, accepted 6 May 2026, online since 16 June 2026.

Introduction

Generalized continua have been theoretically investigated since the pioneering works by Piola, see [1,2]. After a long oblivion, the study of generalized continuum theories started again in the early twentieth century, when a number of mathematicians and mechanicians began questioning the adequacy of classical Cauchy continua to describe microstructured materials with multiple length scales. One of the earliest systematic treatments was provided by the Cosserat brothers, who formulated a theory capable of incorporating independent rotations of material points. Their pioneering monograph "Théorie des corps déformables" [3] laid the foundation for what would later be called Cosserat or micropolar continua. Their work remained ahead of their time and was not fully appreciated until the mid-twentieth century, when the rise of materials with significant microstructural effects revived interest in enriched continuum theories. A major modern push began with the emergence of micromorphic and microstretch theories, most prominently formulated by Mindlin, whose contributions remain central to the field. In a sequence of influential works, albeit sometimes underestimated, Mindlin developed strain-gradient and microstructure-dependent models that generalized classical elasticity by incorporating additional kinematic variables and higher-order gradients. His comprehensive treatment can be found, among others, in [4,5]. These works triggered a sustained development of generalized continuum models across applied mathematics and engineering. Mindlin did base his postulation scheme on variational principles.

Following Mindlin's influence, Eringen unified several micropolar and micromorphic theories into a coherent framework. His monograph provides a definitive exposition, see [6]. Eringen and his collaborators helped to solidify generalized continua as a distinct field within continuum mechanics. Unfortunately, Eringen's approach presents some epistemological flaws, as it is based on the multiplication of postulates (one balance law for each kinematical independent descriptor) and on the presence of serious compatibility problems among the many different constitutive equations to be introduced for "closing" the problem of the determination of the system's evolution equations.

Around the same period, aeroelastic and structural applications motivated further generalizations, including strain-gradient theories formulated by Toupin, whose work preceded and influenced many later developments, see [7]. Richard Toupin did formulate unifying variational principles and therefore did not have the logical and postulation problems present in Eringen's approach. Similarly, Paul Germain [8] made seminal contributions to the development of microstructured continuum mechanics by extending classical theories to incorporate internal degrees of freedom within material elements. He systematically employed the principle of virtual power, as inspired by Lagrange, to deduce consistent balance laws, constitutive equations and boundary conditions for continua endowed with micro-rotations, couple stresses, and internal variables, thus providing a rigorous and unifying variational foundation. Within this framework, he clarified how microstructural effects must be incorporated into the governing equations while preserving fundamental principles such as objectivity and invariance [9].

Germain's formulations established the basis for micropolar, micromorphic, and second-gradient theories, connecting classical elasticity with the nonclassical models first envisioned by the Cosserat brothers. Germain's ideas made it possible to model materials with complex internal architecture, such as composites, granular materials, and modern metamaterials, by incorporating micro-rotations and higher-order stresses into the constitutive structure. His distinctions between hyper-stresses and classical stresses resolved longstanding interpretative ambiguities and anticipated central features of today's gradient and micromorphic models.

The modern translation and presentation of his second-gradient theory in *Mathematics and Mechanics of Complex Systems* [9] has further emphasized the lasting relevance of his ideas and methods, while subsequent authors have highlighted the far-reaching influence of his approach on contemporary generalized continuum mechanics [10,11].

The above-mentioned theories were developed by following approaches postulated directly at the macroscopic scale. The various generalized continuum descriptions that have been established are theoretically well-founded, but they postulate the existence of suitable additional kinematic descriptor(s). In other words, the precise link between the microstructure and the considered kinematic descriptor(s) is missed. The practical consequence is that, for a given known microstructure, the relevant generalized continuum description is not specified, and the effective parameters can only be conjectured. One could say, somewhat provocatively, that while theories exist, we do not know to which specific materials and under what particular conditions they apply. In fact, it has long been questioned if these generalized continua were describing actual mechanical systems. To remedy this shortfall, instead of accepting *a priori* the existence of additional kinematic descriptor(s), an alternative approach has been developed to derive generalized continua by means of a rigorous micro-macro up-scaling procedure. For this purpose, the well-founded asymptotic homogenization method has been proved to be an efficient theoretical tool both in its more standard framework [12–14] and when extended to higher order models [15,16] or discrete structures [17–19]. The benefits of this approach are: (i) to explicitly relate the nature of the generalized description to the microstructure; (ii) to formulate the conditions in which the standard Cauchy model fails to describe the phenomena; (iii) to provide the calculation procedure of the effective parameters; (iv) to improve the physical understanding and facilitate the design of non-conventional synthetic materials often referred to as architectured media or metamaterials. Homogenization-based models give specific examples of generalized continua for specific materials whose microstructure is precisely described. Conversely, the wider problem of the synthesis of the microstructures corresponding to a class of generalized continua demands the determination of a class of microstructures that produces, via homogenization, the chosen continua. Hence, the homogenization method gives a decisive tool for solving the synthesis problem.

In recent decades, generalized continuum mechanics has expanded far beyond its original formulations. Related research flourished within the context of metamaterials, where size effects and internal architecture necessitate enriched continuum descriptions. Contemporary references that synthesize this evolution are, e.g., [20,21]. Today, generalized continuum theories (a general name which includes Cosserat, micromorphic, microstretch, and strain-gradient models) constitute a mature and active area of research, informing the modeling of mechanical metamaterials [22–24], architected solids [25–27], biological tissues [28,29], granular flows [30], and nonlocal damage [31,32]. The historical progression from the Cosserats' conceptual innovation in the early twentieth century to modern gradient and micromorphic formulations demonstrates a continuous effort to bridge the gap between classical continuum descriptions and the complex behavior of real microstructured materials.

A general observation emerges from all these works on higher-order elastic media in static regimes: when a displacement from reference configuration, characterized by one (or more) kinematic variables, can occur with vanishing deformation energy, the elastic energy related to this displacement can only depend on the spatial variation of that variables. For simple homogeneous media, these displacements are only rigid ones. The elastic energy therefore depends on their spatial variation, characterized by the Cauchy–Green tensor, which leads to the standard Cauchy media. For microscopically inhomogeneous media (which exhibit spatial invariance of a representative elementary volume, associated with an internal dimension), accounting for the spatial variation through the Cauchy–Green tensor alone may be insufficient,

and higher-order gradients must then be considered in the formulation of the energy. This is the case for second- (or more) gradient media, where successive gradient terms coexist. In most cases, higher-order terms introduce corrective terms, but they can also be as significant as the first-order terms, see [33,34]. For Cosserat media, rotations are added to the energy-free particle motions, and the description therefore includes rotation gradients. In the case of 1D media such as homogeneous beams, the transverse motion gradient corresponds to a homogeneous beam-section rotation which has vanishing deformation energy. The elastic energy thus depends on the double gradient, i.e., on the curvature, which corresponds to the deformation measure in the Euler beam. But in extension, the energy remains related to simple gradient, as in Cauchy media.

More complex micro-structured media allow for descriptions in which only higher-order gradients are involved (for certain variables). This occurs when the microstructure permits energy-free displacements other than rigid-body motions, which corresponds to the presence of an internal mechanism. Pantographic plates and shells [35,36], characterized by the fact that the deviatoric component of the deformations corresponds to a free-energy mode, or "floppy mode", were the first examples studied in this context. These works followed the pioneering article [37] showing that pantographic beams are second-order gradient media in extension and bending. More recently, a study of media in which the "floppy mode" is associated with the isotropic part of the deformations can be found in [38]. Following the same line of thought, one can expect to obtain a third-gradient beam when the microstructure admits a floppy mode associated with curvature, i.e., a deformation with constant curvature occurs without deformation energy. This is precisely the distinctive feature of the one-dimensional periodic microstructure composed of articulated bi-parallelograms, presented under the name ZAPAB in [39–41] and depicted in Figure 1. This object provides a concrete answer to the quest for third-gradient media that are neither an improvement nor a regularization of second-gradient media, but whose third-gradient description defines their very nature. This study, together with recent works on third gradient media, e.g. [42–45], contributes to understand their features and to progress in solving the wide problem of metamaterial synthesis, which aims to identify microstructures that, once homogenized, obey the generalized continuum model chosen *a priori*; see [46].

The aim of this paper is, by means of a homogenization procedure inspired by the homogenization of discrete media [17,18], to derive the effective third gradient macroscopic description of this kind of microstructure.

The first part of the study is devoted to describing the kinematics of the microstructural mechanism (i.e., when each bar keeps its length constant), in order to understand the properties of the so-called "floppy" modes (i.e., with zero deformation energy) of the microstructure and of the corresponding 1D macro continuum. In a Lagrangian description, the analysis is carried out on the elementary module of the microstructure using the internal angle α (see Figure 2), which is immediately recognized to be related to the macro-curvature, see equation (1).

Then, adapting the ideas of the asymptotic homogenization at the leading order to the new class of micro-structures, we determine the homogenized elastic deformation energy stored in a module of the microstructure deformed by a gradient of curvature combined with extension. Applying Hill's principle, this immediately leads to the energy density of the effective 1D continuum. The latter involves three elastic stiffness coefficients related respectively to the gradient of curvature, the elongation, and the coupling of both, whose expressions are explicitly related to the morphology of the module and the stiffnesses of the micro bars. The three effective stiffnesses are shown to depend on the curvature. The energy description is a dominant-order description, in the sense that the higher-order gradients of curvature and elongation are disregarded.

From these results, the effective behavior of the 1D effective continuum is derived following the Euler–Lagrange method of minimization of total energy (elastic and potential). This enables us to determine that the generalized contact forces (in the sense given by Germain and Mindlin)

in the newly introduced 1D continuum are: (i) normal and transverse force, (ii) couples, and (iii) double couples. Moreover, our analysis provides the corresponding balance equations and specifies the normal force and double couple constitutive laws.

The main results of the paper can be outlined as follows:

- the theoretical derivation of the third gradient 1D continuum description of articulated bi-parallelogram microstructures in large in-plane deformation, when the module remains in the regime of small deformations;
- the analytical expression of the three elastic stiffness coefficients as a function of the morphology of the module, the stiffnesses of the micro-bars and the curvature;
- the formulation of the effective macro-behavior in terms of generalized forces with the corresponding macro-balance equations and constitutive laws.

The paper is organized as follows. Section 1 is devoted to the identification of the mechanism configuration with constant curvature of the microstructure. Section 2 deals with the description of the elastic microstructure under macroscopic deformations, considering separately the cases of elongation at constant curvature and gradient of curvature at constant elongation. The proposed approach, inspired by the asymptotic homogenization of discrete media, yields the stored elastic energy in a module and the explicit determination of the effective elastic parameters. In Section 3, starting from the effective density of energy and using the Euler–Lagrange method of energy minimization, the effective model is established. Some numerical examples are also provided and discussed.

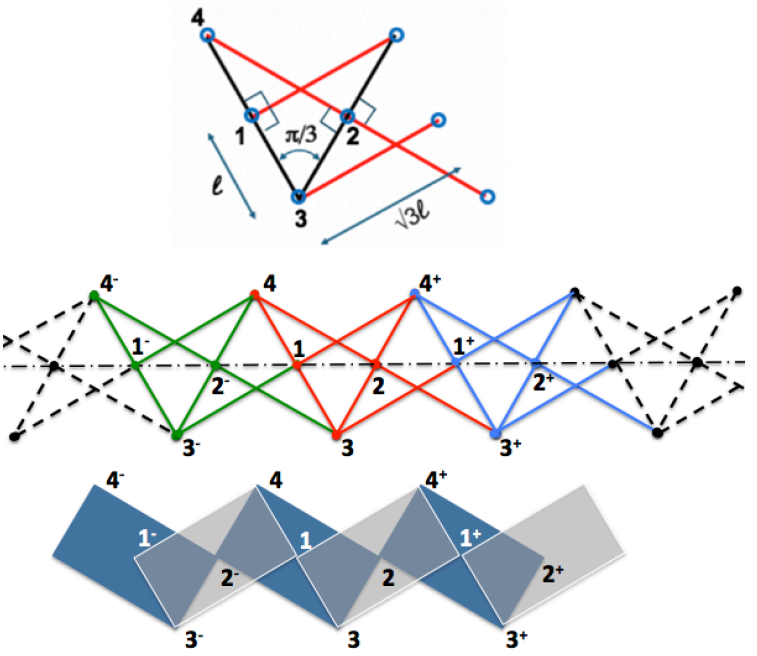

Figure 1. Top: The elementary module made of four short bars of length ℓ and of four long bars of length $\sqrt{3}\,\ell$, articulated at the four hinged nodes ($n = 1,2,3,4$). Center: Periodic articulated bi-parallelogram mechanism in straight configuration. Bottom: Illustration of the two articulated parallelograms (rectangles in straight configuration).

1. Mechanism of constant curvature

1.1. *Topology and geometry*

The specific periodic microstructure, introduced in [39], is based on the elementary module, see Figure 1, bottom. This module is made of four short bars of length ℓ and of four long bars of length $\sqrt{3}\ell$. These bars are connected by hinges, each of them relating two long and two short bars, in such a way that they form the bi-parallelogram articulated microstructured system as depicted in Figure 1 in the straight configuration. The sides of the parallelograms (rectangles in the straight configuration) are the short and long bars and the half diagonal of parallelogram is the short side of the subsequent parallelogram. One can also describe the microstructured system in its straight configuration as an assembly of similar right triangles made of bars (with orthogonal sides ℓ and $\sqrt{3}\ell$, and hypotenuse 2ℓ) which map into one another by symmetry about axis orthogonal to the central line passing through the internal hinges.

Notations

The module contains four hinged nodes which are simply indicated by numbers $\{1,2,3,4\}$. The similar nodes of the subsequent or the preceding modules are respectively denoted as $\{1^+,\dots,4^+\}$ and $\{1^-,\dots,4^-\}$. The distance between two nodes i and j is $|ij|$. A bar connecting nodes i and j (of the same or of an adjacent module) is designed by b_{ij}. A triangle, respectively quadrilateral, of summits the nodes $\{i,j,k\}$, resp. $\{i,j,k,l\}$ is noted $\mathcal{T}_{i,j,k}$, resp. $\mathcal{Q}_{i,j,k,l}$. At a node i, the angle between the two lines relating node i to nodes j and k is noted $\widehat{jik}$. For any vector $\mathbf{v}$, the orthogonal vector in the direct trigonometric sense is denoted $\mathbf{v}^\perp$. Note also that in this paper we will not use the Einstein convention, i.e., repeated indices do not mean summation.

1.2. *One degree of freedom mechanism*

Let us determine the number of degrees of freedom of an isolated elementary module (Figure 1) made up of rigid bars. In the considerations which follow we count the number of the constraint scalar equations to determine the corresponding number of blocked degrees of freedom: the calculation is correct as the system of all these equations has a Jacobian matrix, at each considered configuration, which has maximal rank.

Each isolated rigid bar has three degrees of freedom, two in translation and one in rotation. This gives 24 degrees of freedom for the 8 isolated bars of an isolated elementary module. Since the bars are connected by hinges, we must remove 2 degrees of freedom in translation at each node for each bar connected to another, i.e. $2\times 2=4$ at node 1, $2\times 3=6$ at node 2, $2\times 2=4$ at node 3, 2 at node 4 and 2 at node 4^+. Thus, the total number of degrees of freedom of an isolated module is $24-(4+6+4+4)=6$ degrees of freedom. The latter consist of 3 degrees of freedom of rigid body motion of the module, the 2×1 degrees of freedom of rotation of the bars b_{31^+} and b_{23^+} having a free end, and 1 degree of internal freedom of the module. Indeed, disregarding the two free end's bars, if one of the 6 remaining bars is fixed, the motion of one among the others imposes uniquely the motion of all the others.

Now let us consider two connected modules. They have 2×6 degrees of freedom, from which we must subtract 2 degrees of freedom for each of the three joints common to both modules. Thus, two modules also have $12-3\times 2=6$ degrees of freedom. By the same reasoning, we see that N modules also have 6 degrees of freedom. Thus, without taking into account the two bars that have free ends, the system with rigid bars has one degree of freedom in addition to the three degrees of freedom of the rigid body's movement. Therefore, this system is a single-degree-of-freedom mechanism.

1.3. *Identification of mechanism configurations of constant curvature*

This section aims at identifying the mechanism configurations. They correspond to modes of deformation in which all the bars move as a rigid body, so that since the bars are not deformed, these modes occur without energy.

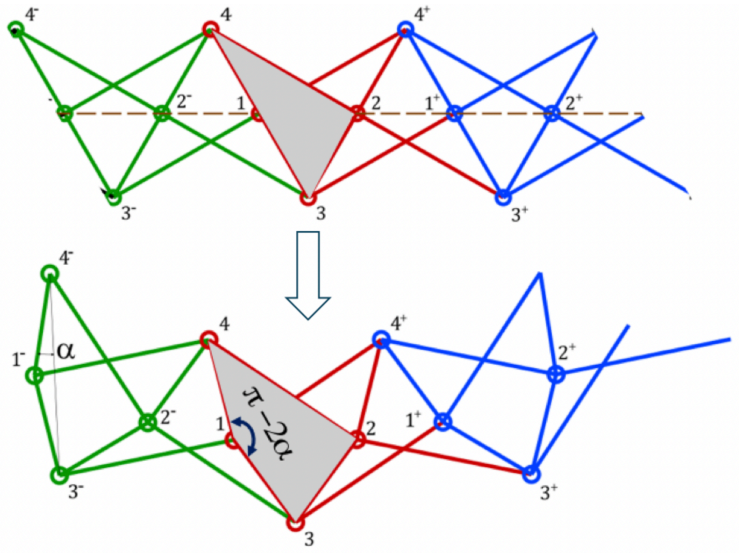

Figure 2. Module modified by introducing angle $\pi - 2\alpha$ at node 1.

Consider the triangle $\mathscr{T}_{2,4,3}$ whose hypotenuse $\{3,4\}$ contains node 1 in the straight configuration. Transform $\mathscr{T}_{2,4,3}$ into a quadrilateral $\mathscr{Q}_{2,4,1,3}$ that preserves the length of each bar, see Figure 2. At node 1, bars b_{13} and b_{14} then form an angle $\widehat{314} = \pi - 2\alpha$, and the distance $|34|$ between nodes 3 and 4 becomes $|34| = 2\ell\cos(\alpha)$. The triangle $\mathscr{T}_{3,2,4}$ whose hypothenuse is thus no longer materialized by bars, becomes not right-angled, and at node 2, the angle $\widehat{324} = \frac{\pi}{2} - \beta$ between bars b_{23} and b_{24} is given by the following relation between sides and angles:[1]

$$\big(2\ell\cos(\alpha)\big)^2 = \ell^2 + (\sqrt{3}\,\ell)^2 - 2\sqrt{3}\,\ell^2\cos\left(\frac{\pi}{2} - \beta\right) \quad \text{thus} \quad \sin(\beta) = \frac{2}{\sqrt{3}}\sin^2(\alpha).$$

Similarly the angles $\widehat{432} = \frac{\pi}{3} + \gamma$ at node 3, and $\widehat{243} = \frac{\pi}{6} + \delta$ at node 4, are deduced from the following relations:

$$(\sqrt{3}\,\ell)^2 = \big(2\ell\cos(\alpha)\big)^2 + \ell^2 - 4\ell^2\cos(\alpha)\cos\left(\frac{\pi}{3} + \gamma\right) \quad \text{thus} \quad \cos\left(\frac{\pi}{3} + \gamma\right) = \frac{2\cos^2(\alpha) - 1}{2\cos(\alpha)},$$

$$\ell^2 = \big(2\ell\cos(\alpha)\big)^2 + (\sqrt{3}\,\ell)^2 - 4\sqrt{3}\,\ell^2\cos(\alpha)\cos\left(\frac{\pi}{6} + \delta\right) \quad \text{thus} \quad \cos\left(\frac{\pi}{6} + \delta\right) = \frac{2\cos^2(\alpha) + 1}{2\sqrt{3}\cos(\alpha)},$$

and finally we have the relation between the angles of $\mathscr{Q}_{2,4,1,3}$:

$$\widehat{132} + \widehat{324} + \widehat{241} + \widehat{413} = 2\pi \quad \text{thus} \quad \gamma + \delta = \beta.$$

[1] In a triangle of sides a, b, c of opposite angle α to the side a one has: $a^2 = b^2 + c^2 - 2bc\cos(\alpha)$.

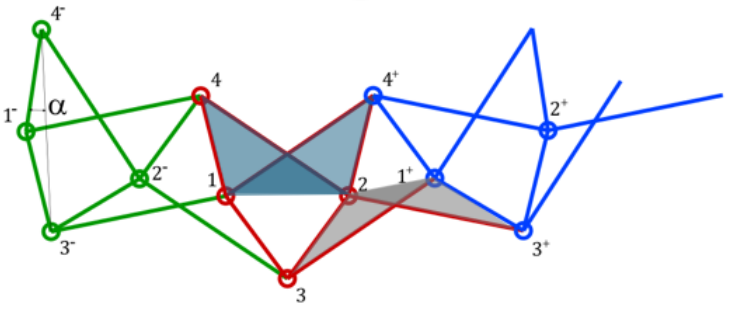

Figure 3. Congruence of triangles $\mathscr{T}_{1,2,4}$ and $\mathscr{T}_{1,2,4^+}$ and of triangles $\mathscr{T}_{3,1^+,2}$, $\mathscr{T}_{3^+,1^+,2}$.

Furthermore, the original rectangle $\mathscr{Q}_{3,2,4,2^-}$ transforms into a parallelogram with alternating angles $\frac{\pi}{2}-\beta$ (at nodes 2 and 2^-) and $\frac{\pi}{2}+\beta$ (at nodes 3 and 4). The parallelogram's diagonal length between nodes 2^- and 2, namely $|2^-2| = 2\ell_\alpha$ is given by the relation

$$(2\ell_\alpha)^2 = \ell^2 + (\sqrt{3}\,\ell)^2 - 2\sqrt{3}\,\ell^2\cos\left(\frac{\pi}{2}+\beta\right) = 4\ell^2\left(1+\frac{\sqrt{3}}{2}\sin(\beta)\right) \quad \text{so} \quad 2\ell_\alpha = 2\ell\sqrt{1+\sin^2(\alpha)}.$$

From the congruence of the triangles $\mathscr{T}_{1,2,4}$ and $\mathscr{T}_{1,2,4^+}$ (see Figure 3) one deduces the angles' equality $\widehat{421} = \widehat{214^+}$ and as the triangle $\mathscr{T}_{1,3,2}$ is isosceles, the angle formed by bars b_{13} and b_{14^+} at node 1 is the same than that formed by bars b_{23} and b_{24} at node 2, i.e.

$$\widehat{314^+} = \widehat{324} = \pi/2 - \beta.$$

Consequently, $\mathscr{Q}_{3,1^+,4^+,1}$ is a parallelogram congruent to $\mathscr{Q}_{3,2,4,2^-}$ with alternating angles $\frac{\pi}{2}-\beta$ (at nodes 1 and 1^+) and $\frac{\pi}{2}+\beta$ (at nodes 3 and 4^+), and $|11^+| = |2^-2| = 2\ell_\alpha$.

The same reasoning applied to triangles $\mathscr{T}_{3,1^+,2}$, $\mathscr{T}_{3^+,1^+,2}$ and $\mathscr{T}_{2,4^+,1^+}$ yields that at node 2 the angle formed by bars b_{23^+} and b_{24^+} are given by

$$\widehat{3^+24^+} = \widehat{31^+4^+} = \pi/2 + \beta.$$

Therefore, parallelograms $\mathscr{Q}_{3^+,2^+,4^+,2}$ and $\mathscr{Q}_{3,2,4,2^-}$ are congruent.[2] In addition, the bars $b_{4^+1^+}$ and b_{13} are parallel, the latter being rotated by an angle 2α compared to b_{41}. This shows that the position of the two bars $\{b_{1^+4^+}, b_{1^+3^+}\}$ of the subsequent modulus is obtained from the position of the two bars $\{b_{14}, b_{13}\}$ of the central modulus through a rigid-body motion, since neither bar length nor relative orientation changes. This rigid body motion consists of a 2α rotation and a translation by distance $2\ell_\alpha$ along the diagonal 11^+ of the parallelogram $Q_{1,3,1^+,3^+}$. Repeating a series of N identical rotation-translations constructs the kinematics of a stress-free periodic mechanism configuration of a microstructured system formed by N modules.

Furthermore, nodes $(1,2,1^+,2^+)$ are cocircular because the angles $\widehat{1,2,2^+}$ and $\widehat{1,1^+,2^+}$ are identical (cf. Figure 3), and this property repeats identically (i.e., with the same angles) for each module of the mechanism. Consequently all type-1 and type-2 nodes lie on the same circle, so the mechanism configuration has constant curvature, see Figure 4. Since each increment $2\ell_\alpha$ undergoes a rotation 2α, it follows that the radius of the circle is:

$$2R_\alpha^2\big((1-\cos(2\alpha)\big) = (2\ell_\alpha)^2 \qquad \Longrightarrow \qquad R_\alpha = \frac{\ell_\alpha}{\sin(\alpha)} = \ell\,\frac{\sqrt{1+\sin^2(\alpha)}}{\sin(\alpha)}. \tag{1}$$

[2] Note also that the triangles $\mathscr{T}_{4,1,2}$ and $\mathscr{T}_{4^+,2,1}$ are congruent and symmetric about the axis $\mathscr{A}_3$ bisector of angle $\widehat{132}$ at node 3. Thus reflecting $\mathscr{Q}_{4,2,3,2^-}$ about $\mathscr{A}_3$ gives $\mathscr{Q}_{1,3,1^+,4^+}$; similarly, reflecting the parallelogram $\mathscr{Q}_{4,2,3,2^-}$ about the axis $\mathscr{A}_4$ bisector of angle $\widehat{142^-}$ at node 4 gives the parallelogram $\mathscr{Q}_{1,4,1^-,3^-}$.

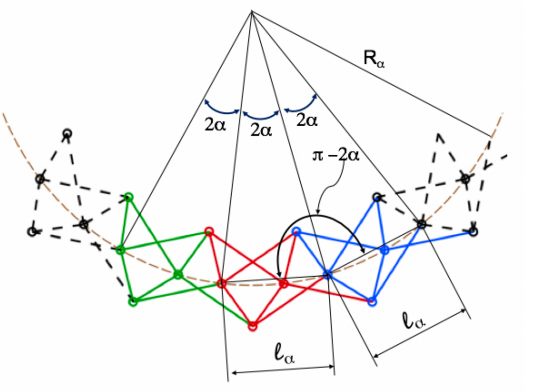

Figure 4. Repetition of the same deformed module by rotation-translation.

1.4. *Positions of the module's nodes under constant curvature*

The previous section shows that the knowledge of the angle α completely determines the transformation of the microstructured system in which the bars undergo rigid body motions. This mechanism characterized by α will be denominated latter by the α-floppy mode or the mechanism configuration.

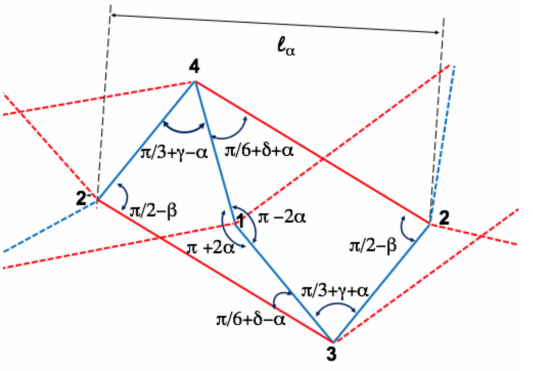

Figure 5. Orientations of the bars of a module in the α-configuration.

The orientation of all bars in the central module is shown in Figure 5. Bars b_{23} and b_{24} rotate by angles γ and δ around node 2, while bars b_{24^+} and b_{23^+} rotate by $2\alpha-\gamma$ and $2\alpha+\delta$ about the same node. Note also that at nodes 1 and 2 the long and short bars each rotate relative to one another by the same angle 2α. Finally, bars b_{31} and $b_{4^+1^+}$ remain parallel while rotating by α.

Under the α-floppy mode, the position P_i of the nodes i in the central module (resp. $P_i^{\pm}$ in the adjacent modules) relatively to the position P_1 (resp. $P_1^{\pm}$) of the reference node 1 (resp. $1^{\pm}$) are given hereafter.

To lighten notations we simply write $\overrightarrow{P_iP_j}$ (or $\overrightarrow{P_iP_j^+}$, etc.) in place of $\overrightarrow{P_iP_j}(\alpha)$. The orientations are referred to the unitary vector $\mathbf{e}_{13}$ of the bar b_{13} in the α-floppy mode configuration. A rotation of angle φ is denoted $\mathbf{R}_\varphi$.

Internal nodes of the central module:

$$\begin{aligned}
&\overrightarrow{P_1P_3} = \ell\mathbf{e}_{13},\\
&\overrightarrow{P_1P_4} = \mathbf{R}_{\pi-2\alpha}\overrightarrow{P_1P_3} = \ell\mathbf{R}_{\pi-2\alpha}\mathbf{e}_{13},\\
&\overrightarrow{P_4P_2} = \sqrt{3}\mathbf{R}_{-\pi+\frac{\pi}{6}+\delta+\alpha}\overrightarrow{P_1P_4} = \sqrt{3}\ell\mathbf{R}_{\frac{\pi}{6}+\delta-\alpha}\mathbf{e}_{13},\\
&\overrightarrow{P_1P_2} = \overrightarrow{P_1P_4} + \overrightarrow{P_4P_2} = \ell\big(\mathbf{R}_{\pi-2\alpha} + \sqrt{3}\mathbf{R}_{\frac{\pi}{6}+\delta-\alpha}\big)\mathbf{e}_{13}.
\end{aligned} \tag{2}$$

Relative nodes position from the central to the subsequent module:

$$\begin{aligned}
&\overrightarrow{P_4^+P_1^+} = \overrightarrow{P_1P_3} = \ell\mathbf{e}_{13},\\
&\overrightarrow{P_1P_4^+} = \sqrt{3}\mathbf{R}_{\frac{\pi}{2}-\beta}\overrightarrow{P_1P_3} = \ell\sqrt{3}\mathbf{R}_{\frac{\pi}{2}-\beta}\mathbf{e}_{13},\\
&\overrightarrow{P_1P_1^+} = \overrightarrow{P_1P_4^+} + \overrightarrow{P_4^+P_1^+} = \ell\big(\sqrt{3}\mathbf{R}_{\frac{\pi}{2}-\beta} + \mathbf{I}\big)\mathbf{e}_{13}.
\end{aligned} \tag{3}$$

Nodes of the adjacent modules:

$$\begin{aligned}
\overrightarrow{P_1^+P_i^+} &= \mathbf{R}_{2\alpha}\overrightarrow{P_1P_i}, \qquad & \overrightarrow{P_1P_1^+} &= \mathbf{R}_{2\alpha}\overrightarrow{P_1^-P_1},\\
\overrightarrow{P_1P_i^+} &= \mathbf{R}_{2\alpha}\overrightarrow{P_1P_i} + \overrightarrow{P_1P_1^+}, \qquad & \overrightarrow{P_1P_i^-} &= \mathbf{R}_{-2\alpha}\overrightarrow{P_1P_i} + \overrightarrow{P_1P_1^-},\\
\overrightarrow{P_iP_j^+} &= \mathbf{R}_{2\alpha}\overrightarrow{P_1P_j} + \overrightarrow{P_1P_1^+} - \overrightarrow{P_1P_i}, \qquad & \overrightarrow{P_iP_j^-} &= \mathbf{R}_{-2\alpha}\overrightarrow{P_1P_j} + \overrightarrow{P_1P_1^-} - \overrightarrow{P_1P_i}.
\end{aligned} \tag{4}$$

From these relations one also deduces that $\overrightarrow{P_iP_i^+} = \mathbf{R}_{2\alpha}\overrightarrow{P_i^-P_i}$.

Tangent vector

The unit vector tangent to the circle passing through the reference points is determined on the reference point P_1 of a given module by

$$\boldsymbol{e}_\theta = \frac{\overrightarrow{P_1^-P_1^+}}{\big\|\overrightarrow{P_1^-P_1^+}\big\|}. \tag{5}$$

The angle θ is increased of 2α when passing from a module to the next one. Hence, for the n^{th} module in the α-configuration $\theta_n = (n-1)2\alpha + \theta_1$.

Remark 1. In the remainder of the paper the notations $\overrightarrow{P_iP_j}$ or $\overrightarrow{P_iP_{j(\alpha)}}$ and $\boldsymbol{e}_{ij} = \frac{\overrightarrow{P_iP_j}}{\|\overrightarrow{P_iP_j}\|}$ will systematically refer to the position of the nodes and the orientation of the bars of the module in the α-floppy mode.

1.5. *Orders of magnitude — Small angle configurations*

Consider a straight system formed by N modules of total length $L = 2\ell N$. In the α-floppy mode, each module rotates by 2α and the reference nodes (as the nodes 2) lie on a circular arc of central angle $\varphi = 2\alpha N$. The length L_α of the broken-line passing to the reference nodes and the radius of curvature R_α of the central line are respectively

$$L_\alpha = N\ell_\alpha = L\sqrt{1+\sin^2(\alpha)}, \qquad R_\alpha = \frac{\ell_\alpha}{\sin(\alpha)} = \frac{L_\alpha}{2N\sin(\varphi/2N)}.$$

For example, to transform a chain of $N = 10$ modules into a quarter circle ($\varphi = \frac{\pi}{4}$), one must impose $\alpha = \frac{\pi}{80} = 2.25°$; for $N = 30$ modules, $\alpha = 0.75°$ suffices. Thus, very small angles α can induce large displacements.

Note also that the ratio of arc length $R_\alpha \times \varphi$ to the length L_α depends only on α, independently of N:

$$\frac{L_\alpha}{R_\alpha\varphi} = \frac{\sin(\varphi/2N)}{\varphi/2N} = \frac{\sin(\alpha)}{\alpha}.$$

This ratio approaches 1 as α becomes small, meaning $R_\alpha \gg \ell_\alpha$. The orientation of the vector $\overrightarrow{P_1P_1^+}$ of each module then approximates the tangent to the circle passing through the reference nodes. Conversely, when $\alpha = \pi/6$ the reference nodes of the modules form stacked hexagons, e.g. 6 hexagons for 36 modules.[3] For the half angle $\alpha = \pi/12$ one would obtain 3 stacked dodecagons. Hence to approximate the module's orientation by the tangent to the circle, one needs at least $\alpha < \pi/24 \approx 7.5°$, which roughly corresponds to $R > 8\ell$.

Small α-angle configurations

The condition of small angle is necessary to derive an elastic equivalent homogenized continuum model. Indeed it guarantees a scale separation in the sense that a small α implies a radius of curvature much larger than ℓ. At small angle α the general geometric relations simplify as follows:

$$\beta \approx \frac{2}{\sqrt{3}}\alpha^2; \qquad \delta \approx \frac{\beta}{4}; \qquad \gamma \approx \frac{3\beta}{4}; \qquad 2\ell_\alpha \approx 2\ell\left(1+\frac{\alpha^2}{2}\right); \qquad R_\alpha \approx \frac{\ell_\alpha}{\alpha} \approx \frac{\ell}{\alpha}\left(1+\frac{\alpha^2}{2}\right).$$

Thus the curvature κ of the α-floppy mode is simply given, up to α^2, by:

$$\kappa = R_\alpha^{-1} \approx \frac{\alpha}{\ell}. \tag{6}$$

Note that the angles β, γ, δ are $O(\alpha^2)$, hence they become all the smaller as α is small. Revisiting the previous examples, for $\alpha = \pi/80$ one has

$$\beta = \frac{2}{\sqrt{3}}\left(\frac{\pi}{80}\right)^2 \approx 0.1°,$$

and for $\alpha = \pi/240$, one finds $\beta \approx 0.01°$. The rectangles therefore remain extremely little deformed even under large displacements. Examples of small α mechanism configurations are presented on Figure 6.

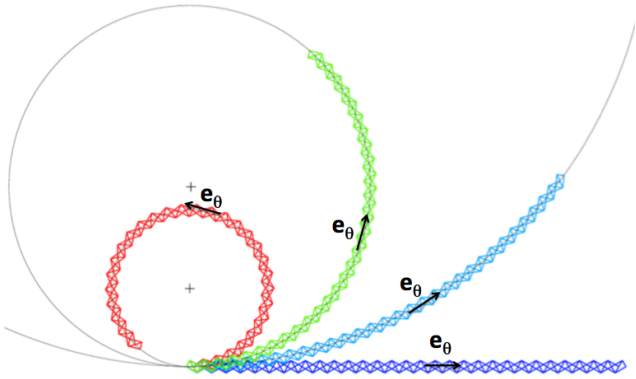

Figure 6. Mechanism's configurations of a microstructured system made of 30 modules, in which ($\alpha = \beta = 0°$), ($\alpha \approx 0.9°$, $\beta \approx 0.0160°$), ($\alpha \approx 2.7°$, $\beta \approx 0.0480°$) and ($\alpha \approx 5.3°$, $\beta \approx 0.5°$). In each case the tangent vector $\mathbf{e}_\theta$ is indicated for the module at the middle of the system.

[3] Such an angle $\alpha = \pi/6$ is close to the angle $\alpha_{\max}$ which would lead to bar b_{13} overlaps with bar b_{2-3}. In that case $\sin(\beta_{\max}) = \frac{\sqrt{3}-1}{2}$ and $\sin^2(\alpha_{\max}) = \frac{\sqrt{3}(\sqrt{3}-1)}{4}$ which gives $\beta_{\max} \approx 21.5°$, $\alpha_{\max} \approx 34°$ and $2\ell_{\alpha_{\max}} \approx 2.3\ell$.

2. Elastic microstructured system subjected to macroscopic deformations

We now consider that the microstructured system undergoes macroscopic deformations that differ from floppy modes. Thus, conversely to the mechanism configuration (in which the bar remains undeformed), the system is subjected to a variation of the curvature and/or of length.

The aim is to derive a 1D effective continuum description of the microstructured system. In this view, we focus on the situation where the microstructured system deformation, which can be large, occurs at a scale much larger than the module's size. This means that from one module to the subsequent the curvature and the length vary incrementally. Consequently, the elastic deformations of the microstructured system subjected to large deformations arises from the small deformations occurring in each module. This enables to treat separately the curvature and length variations, considering variations of curvature at constant length and variation of length at constant curvature. Each of these two scenarios requires a specific homogenization procedure which are described in the two subsequent sections. Applying the principle of superposition in small deformations, one derives the equilibrium state (and the corresponding strain of each bars), of the module undergoing both variations of curvature and of length. Summing the elastic energy of all the bars of the module gives the elastic energy of any deformed module of the microstructured system. The integration of the latter on the whole modules yields the homogenized elastic energy of the whole system, as a function of the gradient of curvature and elongation.

It is crucial to note that, for the considered structure, the "measure" of the separation of scale ratio is fundamentally different from the inverse of the number N of modules forming the microstructure. The correct estimate is given by the ratio of the module size to the radius of curvature, which is directly related to α, see equation (6). Indeed, if we consider, for example, a structure composed of $N = 600$ modules, its deformed structure for $\alpha = \pi/6$ consists of 100 superimposed hexagons. Assuming that the scale ratio is $1/N = 1/600 \approx 1.5 \times 10^{-3}$, one might think that the scales are well separated. This is clearly not the case, because under a small perturbation of this configuration, the change in orientation of one module relative to another cannot be considered incremental, meaning that the scale separation is not respected (the radius of curvature is on the order of the module's size). Conversely, in a structure composed of $N = 10$ modules, in which $\alpha = 0.5^\circ = \ell/R_\alpha \approx 10^{-2}$, a perturbation of this configuration will respect the scale separation much better than the inverse of the number of modules $1/N = 0.1$ would suggest.

In what follows, we will consider small angles α, so that the calculations are performed asymptotically by expanding the trigonometric functions up to $O(\alpha^2)$. This has the advantage of yielding simple algebraic expressions. However, the main reason we restrict ourselves to small values of α is as follows: the continuous model results from the passage from a discrete description to a continuous one using Taylor expansions limited in our case to the first order (for example, finite differences in α are transformed into curvature derivatives), see Section 3. Such a continualization is valid only if the variations from one module to the next can be considered incremental. Consequently, the variation in orientation from one module to the next must be sufficiently small, which implies a very gradual variation in curvature. But since the deformed structure is assumed to be locally a perturbation of the mechanism's α configuration, it follows that, from one cell to the next, the orientation changes by 2α (to within $\mathrm{d}\alpha$). Thus, for the homogenization process to be valid, α must be sufficiently small.

It might be possible to extend the analysis to a finite α, but for now, that question remains open.

2.1. *Macroscopic variation of length at constant curvature*

Let us first focus on the microstructured system when it undergoes a macroscopic length variation under a constant curvature. Then, the configuration of each module departs slightly from

that of the floppy mode having the same curvature. The homogenization procedure allows the determination of the equilibrium of the perturbed state as follows.

- We start by the floppy mode configuration at the curvature corresponding to α. Then, one perturbs the position of the reference nodes $1^{\pm}$ by $\pm\,\mathrm{d}l\,\boldsymbol{e}_\theta^{\pm}$ where $\boldsymbol{e}_\theta^{\pm}$ stands for the unit vector tangent to the circle on the nodes $1^{\pm}$. In this way, the nodes $1^{\pm}$ remain on the same circle with the arc lengths $|11^{+}|$ and $|1^{-}1|$ incremented by $\mathrm{d}l$. Hence the elongation ρ of the module is, up to α^2:
$$\rho = 1 + \frac{\mathrm{d}l}{2\ell_\alpha} \approx 1 + \frac{\mathrm{d}l}{2\ell}. \tag{7}$$
- On the other nodes i, $i \in \{2,3,4,2^{\pm},3^{\pm},4^{\pm}\}$ we add to the floppy mode placement unknown displacements $\mathrm{d}l\,\boldsymbol{\xi}_i$. The scale separation implies a quasi-invariance from a module to the adjacent ones, i.e., along the circle. Hence, the correctors $\mathrm{d}l\,\boldsymbol{\xi}_i$ are identical in adjacent modules provided that they are expressed in the local reference frame of each module. This condition is traduced asymptotically by imposing the local reproducibility (in the sense that both translation and rotation are involved) of the corrector from a module to the adjacent ones. This extends the usual assumption of periodicity which expresses the local invariance by translation only.
- According to the new perturbed positions of the nodes $1^{\pm}$, the corrector in the subsequent module is the corrector of module translated by $\overrightarrow{P_1P_1^{+}} + \mathrm{d}l\,\boldsymbol{e}_\theta^{+}$, and rotated by 2α. Similarly, the corrector in the precedent module is the corrector of module translated by $\overrightarrow{P_1P_1^{-}} - \mathrm{d}l\,\boldsymbol{e}_\theta^{-}$, and rotated by -2α.
- We then determine the elongation of all the bars and the normal forces developed in them. This allows to express the equilibrium of the nodes of the module in the perturbed configuration, under the assumption of small deformations within the module.
- The set of equilibrium equations leads to a linear system for the correctors. Solving the equilibrium yields the displacement of the nodes and then the strain of each bars.

2.1.1. *Node placements*

The common reference frame for three consecutive modules has the node 1 as origin and as axes the vectors $\mathbf{e}_{13}$ and $\mathbf{e}_{13}^{\perp}$ of the central module. In the central module the perturbed positions $\mathbf{P}_i$ of the nodes are that determined by the α-floppy mode, plus the corrector displacements $\mathrm{d}l\,\boldsymbol{\xi}_i$ for $i = 2,3,4$ ($\boldsymbol{\xi}_1 = 0$, since node 1 is the reference):
$$\mathbf{P}_1 = 0, \quad \mathbf{P}_i = \overrightarrow{P_1P_i} + \mathrm{d}l\,\boldsymbol{\xi}_i, \quad i = 2,3,4.$$
The positions of the nodes $(1^{\pm},2^{\pm},3^{\pm},4^{\pm})$ of the adjacent module are deduced from those of $(1,2,3,4)$ as follows:
$$\begin{aligned}
\mathbf{P}_1^{+} &= \overrightarrow{P_1P_1^{+}} + \mathrm{d}l\,\boldsymbol{e}_\theta^{+},\\
\mathbf{P}_i^{+} &= \mathbf{P}_1^{+} + \mathbf{R}_{2\alpha}\big(\overrightarrow{P_1P_i} + \mathrm{d}l\,\boldsymbol{\xi}_i\big), \quad i = 2,3,4,\\
\mathbf{P}_1^{-} &= \mathbf{R}_{\pi-2\alpha}\overrightarrow{P_1P_1^{+}} - \mathrm{d}l\,\boldsymbol{e}_\theta^{-},\\
\mathbf{P}_i^{-} &= \mathbf{P}_1^{-} + \mathbf{R}_{-2\alpha}\big(\overrightarrow{P_1P_i} + \mathrm{d}l\,\boldsymbol{\xi}_i\big), \quad i = 2,3,4,
\end{aligned}$$
where $\boldsymbol{e}_\theta^{+} = \mathbf{R}_{2\alpha}\boldsymbol{e}_\theta$ and $\boldsymbol{e}_\theta^{-} = \mathbf{R}_{-2\alpha}\boldsymbol{e}_\theta$, where $\boldsymbol{e}_\theta$ stands for the unitary vector tangent to the circle at the reference node 1, i.e.
$$\boldsymbol{e}_\theta = \frac{\overrightarrow{P_1^{-}P_1^{+}}}{\big\|\overrightarrow{P_1^{-}P_1^{+}}\big\|}.$$
For nodes $(2,3,4,1^{\pm},2^{\pm},3^{\pm},4^{\pm})$, the displacement is proportional to $\mathrm{d}l$ and given by
$$\mathbf{p}_i\,\mathrm{d}l = \mathbf{P}_i - \overrightarrow{P_1P_i}.$$

2.1.2. *Equilibrium of the nodes*

To express the equilibrium of the nodes of the central module, it is necessary to know the relative displacement of the end points (nodes i and j) of the elastic bars b_{ij} induced by the perturbation of length, i.e., $\mathrm{d}l\mathbf{d}_{ij} = \mathrm{d}l(\mathbf{p}_j - \mathbf{p}_i)$. According to the previous results (recall that $\boldsymbol{\xi}_1 = 0$):

$$\mathbf{d}_{ij} = \boldsymbol{\xi}_j - \boldsymbol{\xi}_i, \quad \mathbf{d}_{ij^+} = \boldsymbol{e}_\theta^+ + \mathbf{R}_{2\alpha}\boldsymbol{\xi}_j - \boldsymbol{\xi}_i, \quad \mathbf{d}_{ij^-} = -\boldsymbol{e}_\theta^- + \mathbf{R}_{-2\alpha}\boldsymbol{\xi}_j - \boldsymbol{\xi}_i, \quad i = 1,2,3,4.$$

Consequently, the axial force $\boldsymbol{N}_{ij}$ in the bar b_{ij} of elastic "spring like" stiffness

$$k_{ij} = \frac{(ES)_{ij}}{|b_{ij}|}$$

and of orientation vector $\mathbf{e}_{ij}$ is given by:

$$\boldsymbol{N}_{ij} = k_{ij} d_{ij}\, \mathrm{d}l\mathbf{e}_{ij}, \quad d_{ij} = \mathbf{d}_{ij} \cdot \mathbf{e}_{ij}. \tag{8}$$

Note that as small deformations are assumed these forces are expressed in the α-floppy mode configuration (refer to Section 1.5 for the quasi-orthonormal vector pairs $(\mathbf{e}_{13}, \mathbf{e}_{14^+})$, $(\mathbf{e}_{23^+}, \mathbf{e}_{24+})$, $(\mathbf{e}_{2^-3}, \mathbf{e}_{2^-4})$ defining the bar orientations). The equilibrium of nodes $(1,2,3,4)$ then reads:

$$\begin{aligned}
&\boldsymbol{N}_{13} + \boldsymbol{N}_{14} + \boldsymbol{N}_{14^+} + \boldsymbol{N}_{13^-} = 0,\\
&\boldsymbol{N}_{23} + \boldsymbol{N}_{24} + \boldsymbol{N}_{23^+} + \boldsymbol{N}_{24^+} = 0,\\
&\boldsymbol{N}_{31^+} + \boldsymbol{N}_{32^-} + \boldsymbol{N}_{31} + \boldsymbol{N}_{32} = 0,\\
&\boldsymbol{N}_{41^-} + \boldsymbol{N}_{42^-} + \boldsymbol{N}_{41} + \boldsymbol{N}_{42} = 0.
\end{aligned} \tag{9}$$

2.1.3. *Equilibrium of the module*

Furthermore, the equilibrium of the module (in absence of internal forces) imposes that some of the forces exerted by the previous module be equal to the sum of the forces transmitted to the next module. Hence,

$$\boldsymbol{N}_{1^-4} + \boldsymbol{N}_{2^-4} + \boldsymbol{N}_{3^-1} + \boldsymbol{N}_{2^-3} = \boldsymbol{N}_{14^+} + \boldsymbol{N}_{24^+} + \boldsymbol{N}_{31^+} + \boldsymbol{N}_{23^+}.$$

Consequently the equations of the set (9) are not independent because their sum vanishes identically (indeed for the nodes inside the module $\boldsymbol{N}_{ij} = -\boldsymbol{N}_{ji}$ and $\boldsymbol{N}_{i^-j} = -\boldsymbol{N}_{ji^-}$). Thus one has to solve a linear system of three vectorial balance equations to determine the three unknown vectors $\boldsymbol{\xi}_2, \boldsymbol{\xi}_3, \boldsymbol{\xi}_4$. This system can be written in the following matrix form by expressing successively the force balance in x and y directions of the nodes $1,2,3$:

$$M_\alpha . W = S_{\rho,\alpha}, \quad W = \left[\xi_{4,x}, \xi_{4,y}, \xi_{3,x}, \xi_{3,y}, \xi_{2,x}, \xi_{2,y}\right]^T, \tag{10}$$

where both the matrix M_α and the forcing term $S_{\rho,\alpha}$ depend on α. The resolution of (10) is performed within the small angle assumption by expanding the trigonometric functions up to $O(\alpha^2)$. For instance, when the bars have the same stiffness, i.e. $k_{ij} = k$, the matrix M_α and the forcing term $S_{\rho,\alpha}$ are expressed up to $O(\alpha^2)$ as:

$$M_\alpha = k \begin{bmatrix}
1 & -2\alpha & 1 & 2\alpha & 0 & 0\\
0 & 1 & 0 & 1 & 0 & 0\\
1+\frac{\sqrt{3}}{2}\alpha & -\frac{3}{2}\alpha & 1-\frac{\sqrt{3}}{2}\alpha & -\frac{1}{2}\alpha & -2 & 0\\
\frac{1}{2}\alpha & \frac{3}{2}\alpha & 1+\frac{\sqrt{3}}{2}\alpha & 1-\frac{\sqrt{3}}{2}\alpha & 0 & -2\\
0 & 0 & -2 & 0 & 1-\frac{\sqrt{3}}{2}\alpha & \frac{3}{2}\alpha\\
0 & 0 & 0 & -2 & -\frac{1}{2}\alpha & 1+\frac{\sqrt{3}}{2}\alpha
\end{bmatrix}, \tag{11}$$

$$S_{\rho,\alpha} = k \begin{bmatrix} \sqrt{3}\alpha \\ -\alpha \\ \frac{1}{2}(-1+\sqrt{3}\alpha) \\ -\frac{1}{2}(\sqrt{3}+\alpha) \\ \frac{3}{4}(1+\sqrt{3}\alpha) \\ -\frac{1}{4}(\sqrt{3}+3\alpha) \end{bmatrix}.$$

The determination of $\{\boldsymbol{\xi}_2, \boldsymbol{\xi}_3, \boldsymbol{\xi}_4\}$ yields the equilibrium state of the module under macroscopic variation of length at constant curvature.

2.2. *Macroscopic variation of curvature at constant length*

For macroscopic variation of curvature at constant length we perform the determination of the perturbed state by the following homogenization procedure.

- In a first step, nodes $(1,2,3,4)$ of the central module are placed according to the α-floppy mode kinematics. The nodes $(1^{\pm}, 2^{\pm}, 3^{\pm}, 4^{\pm})$ of the adjacent modules are placed according to the $(\alpha \pm \mathrm{d}\alpha)$-floppy mode. This is consistent with the idea that when the microstructured system undergoes a curvature that varies at large scale, locally the configuration of each module departs only slightly from that of the floppy mode having the same curvature. Such an increment in angle α corresponds to an increment of the curvature, namely:
$$\mathrm{d}\alpha = \ell\, \mathrm{d}\kappa, \qquad \frac{\mathrm{d}\kappa}{2\ell_\alpha} \approx \frac{\mathrm{d}\alpha}{2\ell^2}. \tag{12}$$
- Furthermore, the position of the reference nodes $1^{\pm}$ of the adjacent modules is placed so that the vector $\overrightarrow{P_1P_1^+}$ is the vector defined by the α-floppy mode, and the vector $\overrightarrow{P_1^-P_1}$ is the vector defined by the $(\alpha - \mathrm{d}\alpha)$-floppy mode. This expresses the fact that the deformation occurs asymptotically at constant length.
- We superpose on the above defined node placements unknowns internal relative displacements $\ell\, \mathrm{d}\alpha\, \boldsymbol{\eta}_i$. As previously, the assumption of scale separation implies that the correctors $\ell\, \mathrm{d}\alpha\, \boldsymbol{\eta}_i$ are identical in adjacent modules provided that they are expressed in the local reference frame of each module. Hence the usual assumption of periodicity is adapted by imposing the local reproducibility (in the sense that both translation and rotation are involved) of the corrector from a central module to the adjacent ones.
- According to the positions of nodes $1^{\pm}$, the corrector in the subsequent module is the corrector of central module translated by $\overrightarrow{P_1P_1^+}$, and rotated by $2\alpha + \mathrm{d}\alpha$. Similarly, the corrector in the precedent module is the corrector of central module translated by $\overrightarrow{P_1P_1^-}$, and rotated by $2\alpha - \mathrm{d}\alpha$. Note that the rotation of the corrector for passing from the central module (in α configuration) to the adjacent modules (in $\alpha \pm \mathrm{d}\alpha$ configuration) is the mean rotation that would occur in the α-floppy mode and the $(\alpha \pm \mathrm{d}\alpha)$-floppy mode, namely $\frac{1}{2}\big(2\alpha + 2(\alpha \pm \mathrm{d}\alpha)\big) = 2\alpha \pm \mathrm{d}\alpha$.
- We then are able to determine the elongation of the bars and the normal forces developed in them. This allows to express the equilibrium of the nodes of the central module (under the assumption of small deformations within the module).
- The set of equilibrium equations yields a linear system for the correctors $\boldsymbol{\eta}_i$. Solving the equilibrium yields the explicit displacement of the nodes and the strain of the bars.

2.2.1. *Node placements*

We choose a common reference frame for three consecutive modules. The origin is the node 1 of the central module, and the axes $\mathbf{e}_{13}$ (along the bar b_{13}) and $\mathbf{e}_{13}^{\perp}$. The perturbed positions $\mathbf{P}_i$

of the nodes $(1,2,3,4)$ of the central module are given by the α-floppy mode placement, plus the corrector $\ell\,\mathrm{d}\alpha\,\boldsymbol{\eta}_i$ for $i=2,3,4$ (with $\boldsymbol{\eta}_1=0$, since node 1 is the reference):

$$\mathbf{P}_1=0,\quad \mathbf{P}_i=\overrightarrow{P_1P_i}+\ell\,\mathrm{d}\alpha\,\boldsymbol{\eta}_i,\quad i=2,3,4.$$

The positions of the nodes $(1^+,2^+,3^+,4^+)$ in the next module, under the curvature parameter $\alpha+\mathrm{d}\alpha$, follow from those of $(1,2,3,4)$ by a rotation of angle $2\alpha+\mathrm{d}\alpha$ about node 1^+ and by a translation, i.e.,

$$\begin{aligned}\mathbf{P}_1^+&=\overrightarrow{P_1P_1^+},\\ \mathbf{P}_i^+&=\mathbf{P}_1^+ +\mathbf{R}_{(2\alpha+\mathrm{d}\alpha)}\big(\overrightarrow{P_1P_{i\,(\alpha+\mathrm{d}\alpha)}}+l\,\mathrm{d}\alpha\boldsymbol{\eta}_i\big),\quad i=2,3,4.\end{aligned}$$

The positions of the nodes $(1^-,2^-,3^-,4^-)$ in the previous module, under curvature parameter $\alpha-\mathrm{d}\alpha$, follow from those of the nodes $(1,2,3,4)$ by a rotation of angle $-(2\alpha-\mathrm{d}\alpha)$ about node 1:

$$\begin{aligned}\mathbf{P}_1^-&=\mathbf{R}_{\pi-(2\alpha-\mathrm{d}\alpha)}\big(\overrightarrow{P_1P_{1\,(\alpha-\mathrm{d}\alpha)}^+}\big)\\ \mathbf{P}_i^-&=\mathbf{P}_1^- +\mathbf{R}_{-(2\alpha-\mathrm{d}\alpha)}\big(\overrightarrow{P_1P_{i\,(\alpha-\mathrm{d}\alpha)}}+l\,\mathrm{d}\alpha\boldsymbol{\eta}_i\big),\quad i=2,3,4.\end{aligned}$$

Note that neglecting $\mathrm{d}\alpha^2$

$$\begin{aligned}\mathbf{R}_{(2\alpha+\mathrm{d}\alpha)}\overrightarrow{P_1P_{i\,(\alpha+\mathrm{d}\alpha)}}-\mathbf{R}_{2\alpha}\overrightarrow{P_1P_{i\,(\alpha)}}&\approx\mathbf{R}_{2\alpha}\big(\mathbf{R}_{\mathrm{d}\alpha}\overrightarrow{P_1P_{i\,(\alpha)}}+\overrightarrow{P_1P_{i\,(\alpha+\mathrm{d}\alpha)}}-\overrightarrow{P_1P_{i\,(\alpha)}}\big)\\ &=\mathbf{R}_{2\alpha}\left(\overrightarrow{P_1P_{i\,(\alpha)}^{\perp}}+\frac{\partial}{\partial\alpha}\overrightarrow{P_1P_{i\,(\alpha)}}\right)\mathrm{d}\alpha\end{aligned}$$

and similarly

$$\mathbf{R}_{-(2\alpha-\mathrm{d}\alpha)}\overrightarrow{P_1P_{i\,(\alpha-\mathrm{d}\alpha)}}-\mathbf{R}_{-2\alpha}\overrightarrow{P_1P_{i\,(\alpha)}}=\mathbf{R}_{-2\alpha}\left(\overrightarrow{P_1P_{i\,(\alpha)}^{\perp}}-\frac{\partial}{\partial\alpha}\overrightarrow{P_1P_{i\,(\alpha)}}\right)\mathrm{d}\alpha.$$

For any node, the small displacement is proportional to $\ell\,\mathrm{d}\alpha$ and given by

$$\mathbf{q}_i\ell\,\mathrm{d}\alpha=\mathbf{P}_i-\overrightarrow{P_1P_i},\quad i=1,2,3,4,1^{\pm},2^{\pm},3^{\pm},4^{\pm}.$$

2.2.2. *Equilibrium state*

From the nodes positions, neglecting the terms in $\mathrm{d}\alpha^2$, the relative displacement of the end nodes i and j of the elastic bars b_{ij}, namely $\ell\,\mathrm{d}\alpha\,\mathbf{h}_{ij}=\ell\,\mathrm{d}\alpha\,(\mathbf{q}_j-\mathbf{q}_i)$ are given by:

$$\begin{aligned}\mathbf{h}_{ij}&=\boldsymbol{\eta}_j-\boldsymbol{\eta}_i,\\ \mathbf{h}_{ij^+}&=\mathbf{R}_{2\alpha}\left(\frac{1}{\ell}\left(\overrightarrow{P_1P_{i\,(\alpha)}^{\perp}}+\frac{\partial}{\partial\alpha}\overrightarrow{P_1P_{i\,(\alpha)}}\right)\right)+\mathbf{R}_{2\alpha}\boldsymbol{\eta}_j-\boldsymbol{\eta}_i,\\ \mathbf{h}_{ij^-}&=\mathbf{R}_{-2\alpha}\left(\frac{1}{\ell}\left(\overrightarrow{P_1P_{i\,(\alpha)}^{\perp}}-\frac{\partial}{\partial\alpha}\overrightarrow{P_1P_{i\,(\alpha)}}\right)\right)+\mathbf{R}_{-2\alpha}\boldsymbol{\eta}_j-\boldsymbol{\eta}_i.\end{aligned}$$

Then, the axial forces $\boldsymbol{N}_{ij}$ in the bars b_{ij} of elastic stiffness k_{ij} and orientation vector $\mathbf{e}_{ij}$ are expressed in the α-floppy mode configuration consistently with the small deformations assumption as

$$\boldsymbol{N}_{ij}=k_{ij}h_{ij}\mathbf{e}_{ij}.\ell\,\mathrm{d}\alpha,\quad h_{ij}=\mathbf{h}_{ij}\cdot\mathbf{e}_{ij}.$$

The set of equilibrium equations at nodes $(1,2,3,4)$ is the same as equation (9). For the same argument as for length variation, this leads to a system of six equations for the six unknowns. This system can be write in matrix form

$$M_\alpha.W=S_{\kappa,\alpha},\quad W=\big[\eta_{4,x},\eta_{4,y},\eta_{3,x},\eta_{3,y},\eta_{2,x},\eta_{2,y}\big]^T,$$

where M_α and G_α depend on α. Unsurprisingly, M_α is identical to that established in (11) for determining the $\boldsymbol{\xi}_i$, as it is the linear operator that expresses the equilibrium of the system. As previously, the system is solved within the small angle assumption up to the order α^2 by

expanding the sine and cosine functions. For instance, when the bars have all the same stiffness $k_{ij} = k$, the forcing term $S_{\kappa,\alpha}$ reads:

$$S_{\kappa,\alpha} = \begin{bmatrix} 0 \\ -1 \\ \frac{3}{2}\alpha \\ -1 + \frac{\sqrt{3}}{2}\alpha \\ \frac{1}{4}(\sqrt{3} - 2\alpha) \\ \frac{1}{4}(1 - 2\sqrt{3}\alpha) \end{bmatrix}.$$

The determination of $\boldsymbol{\eta}_2, \boldsymbol{\eta}_3, \boldsymbol{\eta}_4$ yields the equilibrium state of the module under macroscopic variation of curvature at constant length.

2.3. *Elastic energy under both macroscopic variation of length and curvature*

2.3.1. *Elastic energy of the module*

Combining both effects of length and curvature variation, the equilibrium state of the module is described by the position of its nodes perturbed by $\mathbf{w}_i$. Following the principle of superposition in small deformations, one has

$$\mathbf{w}_i = \boldsymbol{\xi}_i \, \mathrm{d}l + \boldsymbol{\eta}_i \, \mathrm{d}\alpha \ell.$$

Recalling that $\mathrm{d}l = 2\ell(\rho - 1)$ and $\mathrm{d}\alpha = \ell \, \mathrm{d}\kappa$, cf. (7) and (12), the variation of length in the bar b_{ij} reads

$$\lambda_{ij} = (\boldsymbol{d}_{ij} \, \mathrm{d}l + \boldsymbol{h}_{ij} \ell \, \mathrm{d}\alpha).\boldsymbol{e}_{ij} = \big(d_{ij}(\rho - 1) + h_{ij}\ell^2(\mathrm{d}\kappa/2\ell)\big)2\ell.$$

Then the elastic energy stored in the 8 bars of the module reads

$$E = \frac{1}{2}\sum_{\{ij\}} k_{ij}\lambda_{ij}^2 = \frac{1}{2}\left(K_\kappa\left(\frac{\mathrm{d}\kappa}{2\ell}\right)^2 + 2H\left(\frac{\mathrm{d}\kappa}{2\ell}\right)(\rho - 1) + K_\rho(\rho - 1)^2\right)2\ell \tag{13}$$

with

$$K_\kappa(\alpha) = 2\ell^6 \sum_{\{ij\}} \frac{k_{ij}}{\ell} h_{ij}^2, \qquad H(\alpha) = 2\ell^4 \sum_{\{ij\}} \frac{k_{ij}}{\ell} d_{ij} h_{ij}, \qquad K_\rho(\alpha) = 2\ell^2 \sum_{\{ij\}} \frac{k_{ij}}{\ell} d_{ij}^2$$

where $\{ij\} = \big(\{13\}, \{31^+\}, \{14\}, \{14^+\}, \{23\}, \{24\}, \{23^+\}, \{24^+\}\big)$.

Thus, under macroscopic variations of curvature and length, the module is driven by the three elastic coefficients, K_κ, H, K_ρ. All of them depend on α. Their unit is N for K_ρ, $\mathrm{N\,m^2}$ for H, and $\mathrm{N\,m^4}$ for K_κ. The coefficient H reveals the coupling between gradient of curvature and extension.

2.4. *Effective elastic parameters*

The above described procedure enables to determine K_κ, H and K_ρ for any (non-zero) value of the bar's stiffness. In the general case, the analytical expressions are extremely heavy. We present hereafter the results obtained for some cases depicted on Figure 7 that disclose the dependence of the elastic parameters with the curvature, the influence of the contrasts in the bar stiffness, the effect of the symmetry or asymmetry in the stiffness distribution in the module. In any case the calculations are performed with an expansion up to $O(\alpha^2)$.

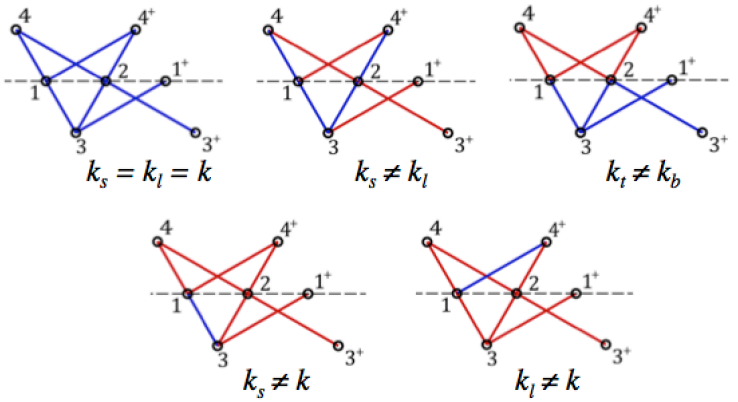

Figure 7. Different types of modules according to the bar's stiffnesses.

2.4.1. *Module with short and long bars of different stiffnesses*

The elastic coefficients of modules made of short bars of stiffnesses k_s and of long bars of stiffnesses k_l are given up to $O(\alpha^2)$ by:

$$K_\kappa = \ell^5 \frac{k_s \cdot k_l}{3k_s + k_l} . \frac{(3k_s + 5k_l)}{4(k_s + 3k_l)}, \qquad H = \ell^3 \frac{\sqrt{3} k_s \cdot k_l}{2(3k_s + k_l)}, \qquad K_\rho = \ell \frac{2k_s \cdot k_l}{3k_s + k_l}. \tag{14}$$

The absence of linear dependence on $\alpha \approx \ell\kappa$, hence on the curvature, implies a quasi-constant value of the elastic parameters when the scale separation is satisfied. The negligible dependence on α is at most quadratic. This is consistent with the "half-module shifted symmetry" of the microstructured system, that implies the same response for positive or negative curvature. Note however — this is not presented here for lack of place — that the local displacement of the nodes presents a linear dependence upon α. Furthermore the fact that $H \neq 0$ reveals that gradient of curvature and extension are actually coupled. As expected the three coefficients are positive, this is also true for the coefficient $G = K_\kappa - H^2.K_\rho^{-1}$ that will be used later on. Expressions (14) simplify as follows in the cases where all the bars are identical and also when either short bars or long bars are rigid:

$$\begin{aligned}
k_l = k_s = k: \quad & K_\kappa = \ell^5 \frac{k}{8}, && H = \ell^3 \frac{k\sqrt{3}}{8}, && K_\rho = \ell \frac{k}{2};\\
k_s \gg k_l: \quad & K_\kappa \to \ell^5 \frac{k_l}{4}, && H \to \ell^3 \frac{k_l}{2\sqrt{3}}, && K_\rho \to \ell \frac{2k_l}{3};\\
k_l \gg k_s: \quad & K_\kappa \to \ell^5 \frac{5k_s}{12}, && H \to \ell^3 k_s \frac{\sqrt{3}}{2}, && K_\rho \to \ell 2k_s.
\end{aligned}$$

As expected, for strong contrasted bars the effective stiffnesses are driven by the weakest bars.

2.4.2. *Module with "top" and "bottom" bars of different stiffnesses*

To investigate the influence of non-symmetry we examine the case where top bars (short and long, i.e., b_{14}, b_{14^+}, b_{24}, b_{24^+}) placed above the central line have stiffness k_T, while the bottom bars (short and long, i.e., b_{31}, b_{31^+}, b_{23}, b_{23^+}) have stiffness k_B, with $\varrho = k_T/k_B$. In that case, up to $O(\alpha^2)$:

$$K_\kappa = \ell^5 \frac{k_B}{4(1+\varrho)}, \qquad H = \ell^3 \frac{k_B\sqrt{3}}{4(1+\varrho)} \left(1 + 2\alpha \frac{1-\varrho}{(1+\varrho)^2}\right), \qquad K_\rho = \ell \frac{k_B}{1+\varrho} \left(1 + \sqrt{3}\alpha \frac{1-\varrho}{1+\varrho}\right).$$

The three stiffnesses are driven by $\frac{k_B}{(1+\varrho)} = \left(\frac{1}{K_B} + \frac{1}{K_T}\right)^{-1}$, i.e. by that of the top and bottom bars in series. In that case, K_κ is constant up to $O(\alpha^2)$, while K_ρ and H depend linearly upon α. Hence, the asymmetry yields a different response in extension for positive or negative curvature (nevertheless the discrepancy is limited as α is small). It is noteworthy that the effects of geometric non-linearity are expressed "within" the effective parameters by their dependence on α.

2.4.3. *Modules with a single bar having a different stiffness from others*

The non-symmetry of modules whose stiffness k_s of a single short bar (resp. k_l of a single long bar) differ from the seven other bars of stiffness k is even more marked. Indeed, in the case of strong contrast between the anomalous and common stiffness one has:

$$
\begin{aligned}
&k_l \gg k: \quad K_\kappa = \ell^5 k \frac{13}{288}(3+\sqrt{3}\alpha), \quad H = \ell^3 k \frac{7\sqrt{3}+10\alpha}{48}, \quad K_\rho = \ell k \frac{15+7\sqrt{3}\alpha}{24};\\
&k_l \ll k: \quad K_\kappa = \ell^5 k \frac{3}{32}(1-\sqrt{3}\alpha), \quad H = \ell^3 k \frac{\sqrt{3}-6\alpha}{16}, \quad K_\rho = \ell k \frac{1-3\sqrt{3}\alpha}{8};\\
&k_s \gg k: \quad K_\kappa = \ell^5 k \frac{5}{96}(3+\sqrt{3}\alpha), \quad H = \ell^3 k \frac{7\sqrt{3}+6\alpha}{48}, \quad K_\rho = \ell k \frac{39+7\sqrt{3}\alpha}{72};\\
&k_s \ll k: \quad K_\kappa = \ell^5 k \frac{1-\sqrt{3}\alpha}{32}, \quad H = \ell^3 k \frac{\sqrt{3}-2\alpha}{16}, \quad K_\rho = \ell k \frac{3-\sqrt{3}\alpha}{8}.
\end{aligned}
$$

In this case, the three effective parameters depend on α, i.e., on the sign of the curvature. In addition, the effective stiffnesses are driven by k, the presence of the anomalous bar is only attested by the change of the numerical coefficients in their expressions. Note however that the case where the anomalous bar is of zero stiffness (or suppressed) cannot be handled in the present framework as this situation would introduce additional degrees of freedom in the system.

Remark 2. As the system is an array of elastic bars, any perturbing deformation of a floppy mode would lead to a positive energy. Hence, the corresponding stiffness must be positive by principle. The fact that they could reach negative value for a range of α would indicate that the approximation made through the homogenization process is erroneous and that the model is not relevant. Note however that in the studied examples a negative value would correspond to a significant angle α. Thus, since the model applies for small values of α the question of possible negative moduli does not arise.

3. Governing equations of the continuous model

In this section we use the homogenization result for establishing and studying the continuous model. In particular we investigate which boundary conditions are admissible given the homogenized energy obtained.

3.1. *From discrete to continuous variables*

Consider a N-modules system whose length is $L = N2\ell$ in the straight configuration aligned along the direction $\boldsymbol{E}_1$ of the orthonormal Cartesian frame $\{O, \boldsymbol{E}_1, \boldsymbol{E}_2\}$. In view of establishing the 1D continuous description we introduce the continuous Lagrangian variable X along $\boldsymbol{E}_1$ and the smooth varying continualized variables $\alpha(X)$, $\theta(X)$, $\kappa(S)$, $\rho(X)$ which describe the deformed configuration. The latter variables are such that for the n^{th} module whose reference node is specified by X_n, $\alpha(X_n) = \alpha_n$, $\theta(X_n) = \theta_n$, $\kappa(X_n) = \kappa_n$, $\rho(X_n) = \rho_n$. Thus, the increments $\mathrm{d}\alpha = \ell\,\mathrm{d}\kappa$ from one module to the next are related to the spatial X-derivatives of the continuous variable

through the Taylor expansion. To obtain a first-order description, it suffices to retain only the first term of the expansion, so that:

$$\mathrm{d}\alpha = 2\ell\nabla\alpha, \qquad \mathrm{d}\kappa = 2\ell\nabla\kappa, \qquad \mathrm{d}\alpha = \ell\,\mathrm{d}\kappa = 2\ell^2\nabla\kappa.$$

Beside, if the first module is oriented according to θ_0 the angle $\theta_n - \theta_0$ of the n^{th} module is the sum of the $2\alpha_i$ angles of the previous modules $i = 1,\ldots,n$, i.e.

$$\theta_n - \theta_0 = \sum_{i=1}^{n} 2\alpha_i = \sum_{i=1}^{n} \frac{2\alpha_i}{2\ell} 2\ell.$$

Changing the Riemann sum into an integral yields the link between the continualized values of α and θ:

$$\theta(X) - \theta(0) = \frac{1}{\ell}\int_0^X \alpha\,\mathrm{d}X$$

which is consistent with

$$\frac{\mathrm{d}\theta}{\mathrm{d}X} = \frac{\alpha(X)}{\ell} = \kappa(X).$$

Hence, while α must be small, θ can take finite large values.

3.2. *Elastic energy of the homogenized microstructured system*

For the N-modules system, the elastic energy is

$$\sum_{n=1}^{N} E_n = \sum_{n=1}^{N} \frac{E_n}{2\ell} 2\ell,$$

where the discrete expression of E_n is given by (13). The density of the elastic energy in the n^{th} module is $E_n/2\ell$. Passing to the continuous limit, the Riemann sum over the number of module is changed in an integral over the length of the system and the increment of curvature is changed into the gradient of the continualized curvature. Thus the elastic energy of the microstructured system, described as a homogenized 1D equivalent continuum has the following Lagrangian expression:

$$\mathscr{E}_e = \frac{1}{2}\int_0^L \left(K_\kappa(\nabla\kappa)^2 + 2H\nabla\kappa(\rho-1) + K_\rho(\rho-1)^2\right)\mathrm{d}X.$$

In the deformed configuration, let us denote by $\boldsymbol{\chi}(X)$ the vector placement of a point of the homogenized system whose reference Lagrangian position is $X\boldsymbol{E}_1$, $0 < X < L$. We have the following geometric relations:

$$\frac{\mathrm{d}\boldsymbol{\chi}}{\mathrm{d}X} = \boldsymbol{\chi}' = \rho\boldsymbol{e}_\theta, \qquad \boldsymbol{e}_\theta = \cos(\theta)\boldsymbol{E}_1 + \sin(\theta)\boldsymbol{E}_2, \qquad \kappa = \frac{\mathrm{d}\theta}{\mathrm{d}X} = \theta', \qquad \nabla\kappa = \frac{\mathrm{d}\kappa}{\mathrm{d}X} = \theta''. \tag{15}$$

Then $\mathscr{E}_e$ is rewritten as

$$\mathscr{E}_e = \frac{1}{2}\int_0^L \left(K_\kappa(\theta'')^2 + 2H\theta''(\rho-1) + K_\rho(\rho-1)^2\right)\mathrm{d}X.$$

3.3. *Minimization of the total energy*

The total energy $\mathscr{E}$ is the sum of the elastic energy $\mathscr{E}_e$ and of the potential of the external forces $\mathscr{U}^{\text{ext}}(\boldsymbol{\chi})$. The latter splits into the potential of the linear body force $\boldsymbol{f}(X)$ ($\mathrm{N\,m^{-1}}$) applied to the homogenized system and the potential $\mathscr{U}_0^L$ of the efforts — to be determined later on — applied at the extremities. That is, recalling that $\boldsymbol{\chi}(X)$ stands for the placement vector:

$$\mathscr{U}^{\text{ext}}(\boldsymbol{\chi}) = \int_0^L -\boldsymbol{\chi}.\boldsymbol{f}\,\mathrm{d}X + \mathscr{U}_0^L.$$

Introducing

$$\boldsymbol{F}(X) = \int_0^L \boldsymbol{f}\,\mathrm{d}X + \boldsymbol{F}(0)$$

we have through integration by parts

$$\int_0^L -\boldsymbol{\chi}.\boldsymbol{f}\,\mathrm{d}X = -\left[\boldsymbol{\chi}.\boldsymbol{F}\right]_0^L + \int_0^L \boldsymbol{\chi}'.\boldsymbol{F}\,\mathrm{d}X = -\left[\boldsymbol{\chi}.\boldsymbol{F}\right]_0^L + \int_0^L \rho\boldsymbol{e}_\theta.\boldsymbol{F}\,\mathrm{d}X; \tag{16}$$

consequently, the total energy takes the form

$$\mathscr{E} = \frac{1}{2}\int_0^L \left(K_\alpha(\theta'')^2 + 2H\theta''(\rho-1) + K_\rho(\rho-1)^2\right)\mathrm{d}X + \int_0^L \rho\boldsymbol{e}_\theta.\boldsymbol{F}\,\mathrm{d}X - \left[\boldsymbol{\chi}.\boldsymbol{F}\right]_0^L + \mathscr{U}_0^L.$$

In order to determine the conditions in which $\boldsymbol{\chi}$ minimizes the total energy, let us determine the first variation of $\mathscr{E}$ according to $\boldsymbol{\chi}$. As the position $\boldsymbol{\chi}(X)$ is fully determined by $\theta(X)$, $\rho(X)$ and the positions at extremities, the variation of $\boldsymbol{\chi}$ is accounted for the variation of these latter variables which have to be considered independently:

$$\delta\mathscr{E} = \int_0^L \left(K_\alpha\theta''\delta\theta'' + H\theta''\delta\rho + H\delta\theta''(\rho-1) + K_\rho(\rho-1)\delta\rho\right)\mathrm{d}X \\ + \int_0^L \left(\delta\rho\boldsymbol{e}_\theta.\boldsymbol{F} + \rho\boldsymbol{e}_\theta^\perp.\boldsymbol{F}\delta\theta\right)\mathrm{d}X - \left[\delta\boldsymbol{\chi}.\boldsymbol{F}\right]_0^L + \delta\mathscr{U}_0^L. \tag{17}$$

First, minimizing $\mathscr{E}$ according to $\delta\rho$ yields:

$$\frac{\delta\mathscr{E}}{\delta\rho}(\delta\rho) = \int_0^L \left(H\theta'' + K_\rho(\rho-1) + \boldsymbol{F}.\boldsymbol{e}_\theta\right)\delta\rho\,\mathrm{d}X + \frac{\delta\mathscr{U}_0^L}{\delta\rho}(\delta\rho) = 0$$

that provides the equations:

$$H\theta'' + K_\rho(\rho-1) + \boldsymbol{F}.\boldsymbol{e}_\theta = 0, \qquad \frac{\delta\mathscr{U}_0^L}{\delta\rho}(\delta\rho) = 0. \tag{18}$$

Thus $\rho-1$ is an internal variable related to θ'' and $\boldsymbol{F}$, and therefore there is no boundary condition associated to ρ. Then minimizing $\mathscr{E}$ according to $\delta\theta$ provides:

$$\frac{\delta\mathscr{E}}{\delta\theta}(\delta\theta) = \int_0^L \left(\left(K_\alpha + H\theta''(\rho-1)\right)\delta\theta'' + \rho\boldsymbol{F}.\boldsymbol{e}_\theta^\perp\delta\theta\right)\mathrm{d}X + \frac{\delta\mathscr{U}_0^L}{\delta\theta}(\delta\theta) = 0.$$

Setting $\mathbb{C} = K_\alpha\theta'' + H(\rho-1)$, one obtains by twice integration by parts:

$$\int_0^L \mathbb{C}\delta\theta''\,\mathrm{d}X = \left[\mathbb{C}\delta\theta'\right]_0^L - \int_0^L \mathbb{C}'\delta\theta'\,\mathrm{d}X = \left[\mathbb{C}\delta\theta'\right]_0^L - \left[\mathbb{C}'\delta\theta\right]_0^L + \int_0^L \mathbb{C}''\delta\theta\,\mathrm{d}X$$

and therefore:

$$\frac{\delta\mathscr{E}}{\delta\theta}(\delta\theta) = \int_0^L \left(\mathbb{C}''\delta\theta + \rho\boldsymbol{F}.\boldsymbol{e}_\theta^\perp\delta\theta\right)\mathrm{d}X + \left[\mathbb{C}\delta\theta'\right]_0^L - \left[\mathbb{C}'\delta\theta\right]_0^L + \frac{\delta U_0^L}{\delta\theta}(\delta\theta)$$

from which one deduces the two equations:

$$\mathbb{C}'' + \rho\boldsymbol{F}.\boldsymbol{e}_\theta^\perp = 0, \qquad \left[\mathbb{C}\delta\theta'\right]_0^L - \left[\mathbb{C}'\delta\theta\right]_0^L + \frac{\delta U_0^L}{\delta\theta}(\delta\theta) = 0. \tag{19}$$

The last equation shows that $\mathbb{C}$ is the dual of $\delta\theta'$ and corresponds therefore to a double couple, while $-\mathbb{C}'$ is the dual of $\delta\theta$ whose physical meaning is a couple. Introducing the couples and double couple applied at the extremities (denoted with an over bar) we have, accounting for the opposite normal at extremities:

$$\left[\mathbb{C}\delta\theta'\right]_0^L = \overline{\mathbb{C}}\big|_0\delta\theta'\big|_0 + \overline{\mathbb{C}}\big|_L\delta\theta'\big|_L, \qquad \left[-\mathbb{C}'\delta\theta\right]_0^L = \overline{C}\big|_0\delta\theta\big|_0 + \overline{C}\big|_L\delta\theta\big|_L.$$

The minimization according to θ and ρ implies the minimization according to $\boldsymbol{\chi}'$. Thus, the only minimization for $\boldsymbol{\chi}$ dealt with its values at the extremities. The latter appears in term $\left[\mathbf{F}.\delta\boldsymbol{\chi}\right]_0^L$ of

the energy. Consequently introducing the forces applied at the extremities (denoted with an over bar) we have:

$$\left[-\mathbf{F}.\delta\boldsymbol{\chi}\right]_0^L = \overline{\mathbf{F}}\big|_0.\delta\boldsymbol{\chi}\big|_0 + \overline{\mathbf{F}}\big|_L.\delta\boldsymbol{\chi}\big|_L.$$

To sum up, the potential $\mathscr{U}_0^L$ of the efforts applied at the extremities reads

$$\mathscr{U}_0^L = \overline{\mathbb{C}}\big|_0\theta'\big|_0 + \overline{\mathbb{C}}\big|_L\theta'\big|_L + \overline{C}\big|_0\theta\big|_0 + \overline{C}\big|_L\theta\big|_L + \overline{\mathbf{F}}\big|_0.\boldsymbol{\chi}\big|_0 + \overline{\mathbf{F}}\big|_L.\boldsymbol{\chi}\big|_L.$$

This expression discloses the natural (force, couple, double couple) or essential (placement, rotation, curvature) boundary conditions that can be applied to the microstructured system.

Remark 3. To apply to the real microstructured system a couple $C = 2\ell F$ one has to impose on a node 1 a force $F\vec{e}_\theta^{\perp}$ and on the node 1^+ a force $-F\vec{e}_\theta^{\perp}$. To apply a double couple $\mathbb{C} = (2\ell)^2 F$, one has to impose on a node 1^- a force $F\vec{e}_\theta^{\perp}$, on the node 1 a force $-2F\vec{e}_\theta^{\perp}$ and on the node 1^+ a force $-F\vec{e}_\theta^{\perp}$. The model can also handle end conditions imposed on the displacement. By construction, the curve given by the 1D continuous model passes through the reference points of each module. This permits to relate the macroscopic and the microscopic position.

3.4. *Balance and constitutive equations*

Equation (18) gives the normal force and its constitutive laws. Furthermore, (19) enables to define the transverse force T, and then the balance of couple C and of double couple $\mathbb{C}$ together with its constitutive law. Hence the microstructured system is governed by the following set of equations, to be completed with the above identified boundary conditions:

$$N + \boldsymbol{F}.\boldsymbol{e}_\theta = 0, \quad N = H\theta'' + K_\rho(\rho - 1), \tag{20}$$

$$T + \boldsymbol{F}.\boldsymbol{e}_\theta^{\perp} = 0, \tag{21}$$

$$-C' + \rho T = 0, \tag{22}$$

$$\mathbb{C}' + C = 0, \quad \mathbb{C} = K_\kappa\theta'' + H(\rho - 1). \tag{23}$$

Note that, according to the definition of N and T, the balance of normal and transverse forces reads

$$N' = \boldsymbol{f}.\boldsymbol{e}_\theta + \theta'\boldsymbol{F}.\boldsymbol{e}_\theta^{\perp}, \qquad T' = \boldsymbol{f}.\boldsymbol{e}_\theta^{\perp} - \theta'\boldsymbol{F}.\boldsymbol{e}_\theta.$$

3.5. *Transverse versus axial deformability*

Let us consider for simplicity a system of length L subjected to small deformations. Then, the kinematic variables θ and ρ defined on (15) are related to the transverse displacement V and axial displacement U by

$$\theta = O\left(\frac{V}{L}\right), \qquad \rho - 1 = O\left(\frac{U}{L}\right).$$

As a result, the order of magnitude the three terms of the elastic energy reads

$$K_\alpha(\theta'')^2 = \mathscr{K}O\left(\ell^5\left(\frac{V}{L^3}\right)^2\right), \qquad 2H\theta''(\rho - 1) = 2\mathscr{K}O\left(\ell^3\frac{V}{L^3}.\frac{U}{L}\right), \qquad K_\rho(\rho - 1)^2 = \mathscr{K}O\left(\ell\left(\frac{U}{L}\right)^2\right).$$

Furthermore, as we saw in Section 2.4, the effective stiffnesses are given by:

$$K_\kappa = \mathscr{K}O(\ell^5), \qquad H = \mathscr{K}O(\ell^3), \qquad K_\rho = \mathscr{K}O(\ell),$$

where $\mathscr{K}$ depends on the set of bar's stiffnesses. This implies that for the three contributions to be of the same order one must have

$$U = O\left(\frac{\ell}{L}\right)^2 V.$$

Consequently, the ratio of axial to transverse displacement is of the same order of magnitude as the square of the inverse of the slenderness ratio (since the thickness of the microstructured system is equal to $\sqrt{3}\ell$). This ratio is significantly smaller than that of an Euler beam, for which it is equal to the inverse of the slenderness ratio. Thus, for the extension energy to be of the same order as the curvature gradient energy, the extension motion must be two orders of magnitude smaller than that induced by a curvature gradient. In other words, when the three terms of the elastic energy are at the same level, the microstructured system can be considered kinematically as quasi-inextensible, even though the extension energy is not negligible. This reflects the fact that K_ρ is much larger than K_κ.

3.6. *Example: deformation induced by couple and double couple*

Consider a microstructured system of length L, unloaded i.e. $\boldsymbol{f} = 0$, free of forces at extremities i.e. $\overline{\mathbf{F}}\big|_0 = \overline{\mathbf{F}}\big|_L = 0$, undergoing the following boundary conditions $\boldsymbol{\chi}\big|_0 = 0$, $\theta\big|_0 = 0$, $\theta'\big|_0 = 0$ and $\mathbb{C}\big|_L = \overline{\mathbb{C}}$, $C\big|_L = \overline{C}$. Then one has $\mathbf{F} = 0$ and consequently:

$$N = H\theta'' + K_\rho(\rho - 1) = 0, \qquad \mathbb{C}'' = \big(K_\alpha\theta'' + H(\rho-1)\big)'' = 0,$$

so that

$$G\theta'''' = 0, \qquad G = K_\kappa - H^2K_\rho^{-1}.$$

With the boundary conditions one deduces that

$$\theta = a\left(\frac{X}{L}\right)^3 + b\left(\frac{X}{L}\right)^2, \qquad \rho = 1 - \frac{H}{K_\rho}\theta'' = 1 - \frac{H}{K_\rho}\left(6a\frac{X}{L} + 2b\right), \tag{24}$$

$$\overline{\mathbb{C}} = G\theta''\big|_L = (6a+2b)G, \qquad \overline{C} = -G\theta'''\big|_L = 6aG/L. \tag{25}$$

Thus

$$a = \frac{\overline{C}L}{6G}, \qquad b = \frac{\overline{\mathbb{C}} - \overline{C}L}{2G},$$

and

$$\theta = \frac{\overline{C}L}{2G}\left(\frac{1}{3}\left(\frac{X}{L}\right)^3 + \left(\frac{\overline{\mathbb{C}}}{\overline{C}L} - 1\right)\left(\frac{X}{L}\right)^2\right), \qquad \rho = 1 - \frac{H}{K_\rho}\frac{\overline{C}}{GL}\left(\frac{X}{L} + \frac{\overline{\mathbb{C}}}{\overline{C}L} - 1\right).$$

Furthermore, $\mathbb{C}(0) = 0$ and $C(0) = \overline{C}$. In particular, when $\overline{C} = 0$, i.e. when only a double couple is applied at the extremity $X = L$, the curvature varies linearly, $\theta' = \frac{\overline{\mathbb{C}}}{G}\frac{X}{L}$, and the elongation is constant, $\rho = 1 - \frac{H}{K_\rho}\frac{\overline{\mathbb{C}}}{GL^2}$. In the general case, the shape of the microstructured system is obtained by integrating the equations $\frac{\mathrm{d}\boldsymbol{\chi}_1}{\mathrm{d}X} = \rho\cos(\theta)$ and $\frac{\mathrm{d}\boldsymbol{\chi}_2}{\mathrm{d}X} = \rho\sin(\theta)$. Figure 8 illustrates the deformed shape for loading values **a**, **b**, **c**, **d**, **e** of $\overline{C}$ and $\overline{\mathbb{C}}$ given in Table 1.

To be valid, these continuous descriptions must satisfy the scale separation condition, which requires $\alpha = \ell\theta' \le \alpha_{\max} = \pi/24$ as discussed in Section 1.5. We can then deduce the following

Table 1.

	Loading				
	a	**b**	**c**	**d**	**e**
$\overline{C}L/6G$	0	2π	π	-2π	-4π
$\overline{\mathbb{C}}/CL$	$\overline{\mathbb{C}} = 4\pi G$	1	2/3	5/6	5/6
$N_{\min}$	48	72	12	48	96

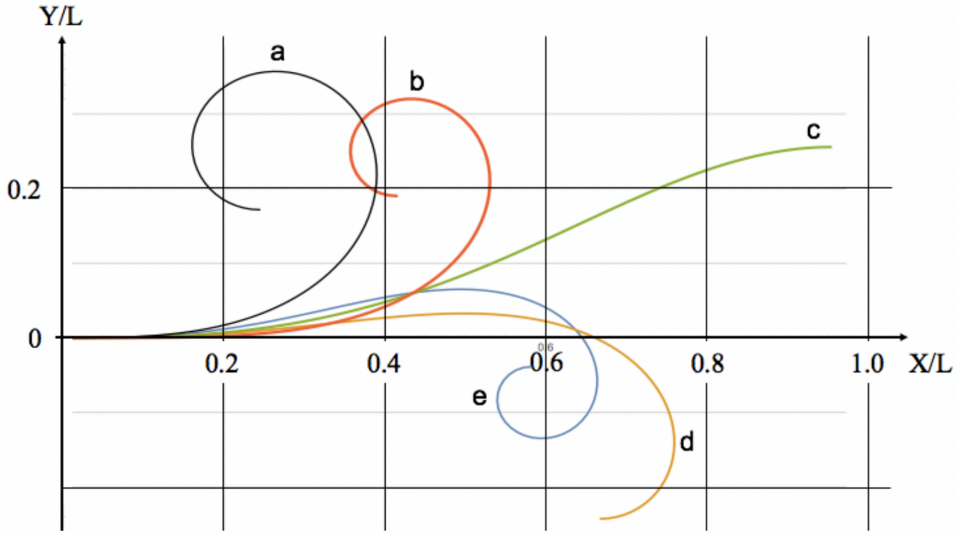

Figure 8. Shape of the microstructured system submitted to several values of $\overline{C}$ and $\overline{\mathbb{C}}$. **a**: $\overline{C}L = 0$, $\overline{\mathbb{C}} = 4\pi G$. **b**–**e**: see Table 1.

restriction, which depends on the applied loading and allows us to estimate the minimum number of modules required for the continuous model to be valid:

$$\alpha = \frac{L}{2N}\theta' = \frac{1}{2N}\frac{\overline{C}L}{2G}\left(\left(\frac{X}{L}\right)^2 + 2\left(\frac{\overline{\mathbb{C}}}{\overline{C}L} - 1\right)\frac{X}{L}\right) \leq \alpha_{\max}.$$

- For the loading **a** where $\overline{C} = 0$, α increases linearly so that for an imposed double couple $\overline{\mathbb{C}} = 4\pi G$,
$$\frac{\overline{\mathbb{C}}}{2G}\frac{1}{N} \leq \alpha_{\max}, \quad N \geq N_{\min} = \frac{\overline{\mathbb{C}}}{2G}\frac{1}{\alpha_{\max}} = 2\pi/(\pi/24) = 48.$$
Hence for this loading, the minimum number of modules for the continuous model to be valid should be $N_{\min} \approx 50$.
- For the loading **b** where $\overline{\mathbb{C}}/CL = 1$, α increases quadratically. In the case where $\overline{C}L/6G = \overline{\mathbb{C}}6G = 2\pi$ we are left with
$$\frac{1}{2N}\frac{\overline{C}L}{2G} \leq \alpha_{\max}, \quad N \geq N_{\min} = \frac{\overline{\mathbb{C}}}{4G}\frac{1}{\alpha_{\max}} = 3\pi/(\pi/24) = 72.$$
- For loadings **c**, **d**, and **e**, the same analysis, based on $\max(\alpha) \leq \alpha_{\max}$, yields the values of $N_{\min}$ shown in Table 1.

Readers may refer to [41], where full numerical simulations have been performed. A more in-depth numerical analysis will be the subject of future articles.

4. Closing remarks and future prospects

In this paper we establish the homogenized energy of the considered articulated bi-parallelogram microstructured systems (ZAPAB) under large in-plane macro-deformation, assuming that the bars constituting the micro-architecture are in a linearized deformation regime. These micro-mechanisms were conceived (see [39,41]) to supply a one parameter family of circular "floppy modes" (i.e. zero deformation energy configurations). The micro-mechanism becomes a micro-structure by adding suitable extra constraints. In this way a natural candidate for a micro-structure producing a third gradient 1D continuum is found.

Indeed, we prove that such periodic micro-structure behave macroscopically as a weakly extensible third gradient 1D continuum, whatever is the choice made for all the positive stiffnesses of the micro bars constituting it.

The effective behavior of homogenized 1D continuum has been identified in two steps.

Inspired by, and slightly generalizing, the basic ideas of the homogenization of discrete media, we have found the homogenized elastic deformation energy stored in a module of a microstructured system deformed by a gradient curvature combined with extension and consequently deduced the energy density of the effective 1D continuum. The slight generalization of the method lies in the fact that instead of considering that the cell and its internal variables are simply translated from one cell to the next one according to the periodicity, we consider that the module and its internal variables are translated and rotated from one module to the next one according to the locally matching floppy mode configuration. The equivalent continuum at the macroscale involves three elastic stiffness coefficients related respectively to the gradient curvature, the elongation and the coupling of both, whose expressions are explicitly related to the morphology of the module and the stiffnesses the micro bars. The three effective rigidities appear as functions of the curvature scaled by the size of the module. The constant coefficients of these functions are the leading terms dominating when the radius of curvature is much larger than the module size. A linear dependence with the curvature arises only for asymmetric bar stiffnesses distribution in the module and induces (slightly) different response for positive or negative curvature, while quadratic term arises for symmetric distribution, making the response very weakly sensitive to the curvature state of the microstructured system.

Having obtained the macro-deformation energy, the effective behavior of the microstructured system has been derived following the Euler–Lagrange method of minimization of total energy, including the elastic deformation energy and the potential energy relative to externally applied admissible loads. The above procedure permits: (i) to disclose the driving generalized forces in terms of normal and transverse force and couple and double couple; (ii) to provide the corresponding balance equations and boundary conditions (so called local strong equilibrium conditions), thus determining naturally the class of external loads applicable to third gradient beams; and (iii) to specify the normal force and double couple constitutive laws. Albeit these results are established by assuming a large scale separation, we expect that already a discrete macrostructure in which the radius of curvature is twenty times the module's length can be replaced effectively with the continuum model.

Let us finally mention worthy issues that deserve to be further investigated.

- Beyond this specific studied case, the adapted homogenization procedure developed in this paper can successfully deal with other structures exhibiting an effective one-dimensional continuum third (may be higher) gradient behavior under large deformations in a plane motion. This will be the topic of future investigations. The homogenization techniques to be developed will be an important part of the perspective solution of several synthesis problems.
- The study of all the boundary layers which may arise in the considered systems could improve the understanding of their mechanical properties.
- The search for analytical or approximated solutions to the above deduced PDEs under different loadings deserve attention, as it will fully exhibit the "exoticity" of newly introduced 1D continua.
- The comparison of the presented theory with experiments, would be of interest to improve the idealized model and eventually modify it for making possible its engineering applications. The newly introduced ZAPAB microstructure can be designed by suitable 3D printing.
- It would be interesting to generalize this model to account for viscoelastic or thermoelastic beams, as well as dynamic effects, and to address situations involving finite angle α.

Acknowledgments

C. Boutin warmly thanks the Profs. F. dell'Isola and F. d'Annibale of the University of L'Aquila and Prof. A. Bersani of Sapienza University of Rome, for funding his sabbatical stay in their research teams and for the fruitful scientific interactions.

Declaration of interests

The authors do not work for, advise, own shares in, or receive funds from any organization that could benefit from this article, and have declared no affiliations other than their research organizations.

References

[1] F. dell'Isola, G. Maier, U. Perego, U. Andreaus, R. Esposito and S. Forest, *The complete works of Gabrio Piola: Volume I*, Advanced Structured Materials, vol. 38, Springer, 2014.

[2] F. dell'Isola, U. Andreaus and L. Placidi, "At the origins and in the vanguard of peridynamics, non-local and higher-gradient continuum mechanics: an underestimated and still topical contribution of Gabrio Piola", *Math Mech Solids* **20** (2015), no. 8, pp. 887–928.

[3] E. Cosserat and F. Cosserat, *Theory of deformable bodies*, Hermann, 1909.

[4] R. D. Mindlin, "Micro-structure in linear elasticity", *Arch. Ration. Mech. Anal.* **16** (1964), pp. 51–78.

[5] R. D. Mindlin, "Second gradient of strain and surface-tension in linear elasticity", *Int. J. Solids Struct.* **1** (1965), no. 4, pp. 417–438.

[6] A. C. Eringen, *Microcontinuum field theories: I. Foundations and solids*, Springer, 2012.

[7] R. A. Toupin, "Elastic materials with couple-stresses", *Arch. Ration. Mech. Anal.* **11** (1962), no. 1, pp. 385–414.

[8] P. Germain, "The method of virtual power in continuum mechanics. Part 2: Microstructure", *SIAM J. Appl. Math.* **25** (1973), no. 3, pp. 556–575.

[9] P. Germain, "The method of virtual power in the mechanics of continuous media, I: Second-gradient theory", *Math. Mech. Complex Syst.* **8** (2020), no. 2, pp. 153–190.

[10] M. Epstein and R. Smelser, "An appreciation and discussion of Paul Germain's "The method of virtual power in the mechanics of continuous media, I: Second-gradient theory"", *Math. Mech. Complex Syst.* **8** (2020), no. 2, pp. 191–199.

[11] S. Forest, "Use and abuse of the method of virtual power in generalized continuum mechanics and thermodynamics", in *Generalized Models and Non-classical Approaches in Complex Materials 1*, Springer, 2018, pp. 311–334.

[12] E. Sánchez-Palencia, *Non-homogeneous media and vibration theory*, Springer, 1980.

[13] N. S. Bakhvalov and G. Panasenko, *Homogenisation: averaging processes in periodic media: mathematical problems in the mechanics of composite materials*, Mathematics and its Applications, vol. 36, Springer, 2012.

[14] J.-L. Auriault, C. Boutin and C. Geindreau, *Homogenization of coupled phenomena in heterogenous media*, John Wiley & Sons, 2009.

[15] C. Boutin and J.-L. Auriault, "Rayleigh scattering in elastic composite materials", *Int. J. Eng. Sci.* **31** (1993), no. 12, pp. 1669–1689.

[16] C. Boutin, "Microstructural effects in elastic composites", *Int. J. Solids Struct.* **33** (1996), no. 7, pp. 1023–1051.

[17] H. Tollenaere and D. Caillerie, "Continuous modeling of lattice structures by homogenization", *Adv. Eng. Softw.* **29** (1998), no. 7–9, pp. 699–705.

[18] A. Raoult, D. Caillerie and A. Mourad, "Elastic lattices: equilibrium, invariant laws and homogenization", *Ann. Univ. Ferrara, Sez. VII, Sci. Mat.* **54** (2008), no. 2, pp. 297–318.

[19] S. Hans and C. Boutin, "Dynamics of discrete framed structures: a unified homogenized description", *J. Mech. Mater. Struct.* **3** (2008), no. 9, pp. 1709–1739.

[20] C. Boutin, "Homogenization methods and generalized continua in linear elasticity", in *Encyclopedia of continuum mechanics* (H. Altenbach and A. Öchsner, eds.), Springer, 2019, pp. 1–35.

[21] H. Altenbach and V. A. Eremeyev, *Generalized continua. From the theory to engineering applications*, CISM International Centre for Mechanical Sciences, vol. 541, Springer, 2012.

[22] B. E. Abali and E. Barchiesi, "Additive manufacturing introduced substructure and computational determination of metamaterials parameters by means of the asymptotic homogenization", *Contin. Mech. Thermodyn.* **33** (2021), no. 4, pp. 993–1009.

[23] I. Giorgio, A. Ciallella and D. Scerrato, "A study about the impact of the topological arrangement of fibers on fiber-reinforced composites: some guidelines aiming at the development of new ultra-stiff and ultra-soft metamaterials", *Int. J. Solids Struct.* **203** (2020), pp. 73–83.

[24] L. Placidi, M. G. El Sherbiny and P. Baragatti, "Experimental investigation for the existence of frequency band gap in a microstructure model", *Math. Mech. Complex Syst.* **9** (2022), no. 4, pp. 413–421.

[25] R. Fedele and D. J. Steigmann, "Lagrangian and Eulerian formulations of second-grade elasticity via convected coordinates", *Math. Mech. Complex Syst.* **13** (2025), no. 3, pp. 377–389.

[26] M. Shirani, I. Giorgio, D. Astori and J. D. Humphrey, "A mixed Cosserat and higher gradient formulation for fibrous tissues and biomaterials", *Int. J. Solids Struct.* **324** (2026), article no. 113671.

[27] E. Barchiesi, "Equilibria of axial-transversely loaded homogenized duoskelion beams", *Math. Mech. Complex Syst.* **12** (2024), no. 3, pp. 283–309.

[28] G. La Valle, C. Soize, A. Misra and I. Giorgio, "A nonlinear micropolar continuum model with diffusion–reaction equation for remodeling of bone with trabecular lattice microarchitecture", *Math Mech Solids* (2026), pp. 1–18. Online first.

[29] R. Allena, D. Scerrato, A. M. Bersani and I. Giorgio, "A bi-dimensional model bridging microdamage evolution and bone remodeling: a computational study on a human femur", *Math. Mech. Complex Syst.* **13** (2025), no. 3, pp. 347–376.

[30] N. Yilmaz, L. Placidi, A. Misra and F. Fabbrocino, "A parametric study on a granular micromechanics continuum-based hemivariational approach: unraveling the emergence of critical states in granular materials", *Math. Mech. Complex Syst.* **13** (2025), no. 1, pp. 25–54.

[31] F. Roscini, N. Rezaei and L. Placidi, "A damage elasto-plastic discrete model for the nonlinear characterization of pullout tests", *Math. Mech. Complex Syst.* **13** (2025), no. 1, pp. 73–97.

[32] A. Scrofani, E. Barchiesi, B. Chiaia, A. Misra and L. Placidi, "Diffusion of a damaging fluid through a dam-shaped bidimensional body for the estimation of its lifetime", *Math. Mech. Complex Syst.* **14** (2025), no. 2, pp. 117–142.

[33] C. Pideri and P. Seppecher, "A second gradient material resulting from the homogenization of an heterogeneous linear elastic medium", *Contin. Mech. Thermodyn.* **9** (1997), no. 5, pp. 241–257.

[34] C. Boutin and J. Soubestre, "Generalized inner bending continua for linear fiber reinforced materials", *Int. J. Solids Struct.* **48** (2011), no. 3–4, pp. 517–534.

[35] C. Boutin, F. dell'Isola, I. Giorgio and L. Placidi, "Linear pantographic sheets: asymptotic micro-macro models identification", *Math. Mech. Complex Syst.* **5** (2017), no. 2, pp. 127–162.

[36] E. Barchiesi, S. R. Eugster, L. Placidi and F. dell'Isola, "Pantographic beam: a complete second gradient 1D-continuum in plane", *Z. Angew. Math. Phys.* **70** (2019), no. 5, article no. 135.

[37] J.-J. Alibert, P. Seppecher and F. dell'Isola, "Truss modular beams with deformation energy depending on higher displacement gradients", *Math Mech Solids* **8** (2003), no. 1, pp. 51–73.

[38] B. Audoly, C. Lestringant and H. Nassar, "Homogenizing elastic lattices with mechanisms", *Eur. J. Mech. A Solids* **117** (2026), article no. 105956 (14 pages).

[39] F. dell'Isola, S. Moschini and E. Turco, "Towards the synthesis of planar beams whose deformation energy depends on the third gradient of displacement", *Math. Mech. Complex Syst.* **12** (2024), no. 4, pp. 573–597.

[40] L. Murcia Terranova, "Planar one-dimensional continua whose energy depends on the gradient of curvature: an overview of their applications in metamaterials design", *Math. Mech. Complex Syst.* **13** (2025), no. 2, pp. 127–166.

[41] L. M. Terranova, E. Turco, A. Misra and F. dell'Isola, "Computational identification of double-bending stiffness: from Zigzagged Articulated Parallelograms with Articulated Braces (ZAPAB) structures to pure-curvature gradient planar inextensible 1D continua", *Comptes Rendus. Mécanique* **353** (2025), no. G1, pp. 647–672.

[42] B. Durand, A. Lebée, P. Seppecher and K. Sab, "Predictive strain-gradient homogenization of a pantographic material with compliant junctions", *J. Mech. Phys. Solids* **160** (2022), article no. 104773.

[43] R. Fedele, "Deformation-induced coupling of the generalized external actions in third-gradient materials", *Z. Angew. Math. Phys.* **73** (2022), article no. 218 (29 pages).

[44] F. dell'Isola and R. Fedele, "Irreducible representation of surface distributions and Piola transformation of external loads sustainable by third gradient continua", *Comptes Rendus. Mécanique* **351** (2023), no. S3, pp. 91–120.

[45] R. Fedele, "Eulerian–Lagrangian transformation of H-forces in generalized elasticity by recursive projection and integration", *Math. Mech. Solids* **31** (2025), no. 6.

[46] F. dell'Isola, D. Steigmann and A. Della Corte, "Synthesis of fibrous complex structures: designing microstructure to deliver targeted macroscale response", *Appl. Mech. Rev.* **67** (2015), no. 6, article no. 060804 (21 pages).